US Army Corps of Engineers

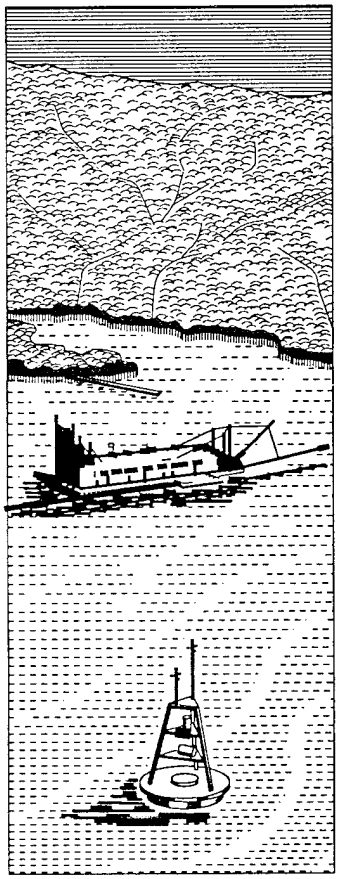

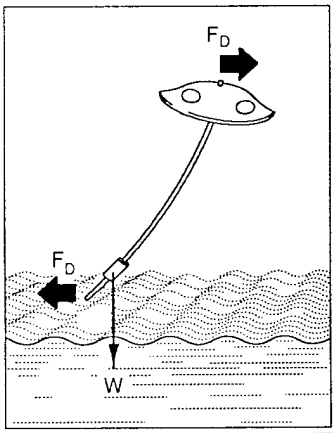

DRRP

DREDGING RESEARCH PROGRAM

TECHNICAL REPORT DRP-94-7

CORRELATING SEABED DRIFTER WEIGHTS TO SAND THRESHOLD CONDITIONS IN WAVE AND WAVE/CURRENT ENVIRONMENTS

by

Edward B. Hands

DEPARTMENT OF THE ARMY
Waterways Experiment Station, Corps of Engineers
3909 Halls Ferry Road, Vicksburg, Mississippi 39180-6199

and

Charles K. Sollitt

O. H. Hinsdale Wave Research Laboratory
Oregon State University
Corvallis, Oregon 97331

December 1994

Final Report

Prepared for DEPARTMENT OF THE ARMY
U.S. Army Corps of Engineers
Washington, DC 20314-1000

Under Work Unit 32467

The Dredging Research Program (DRP) is a seven-year program of the U.S. Army Corps of Engineers. DRP research is managed in these five technical areas:

Area 1 - Analysis of Dredged Material Placed in Open Water
Area 2 - Material Properties Related to Navigation and Dredging
Area 3 - Dredge Plant Equipment and Systems Processes
Area 4 - Vessel Positioning, Survey Controls, and Dredge Monitoring Systems
Area 5 - Management of Dredging Projects

US Army Corps
of Engineers
Waterways Experiment
Station

Dredging Research Program Report Summary

Correlating Seabed Drifter Weights to Sand Threshold Conditions in Wave and Wave/Current Environments (TR DRP-94-7)

ISSUE: About 300 million cu yd of sediment accumulates in the Nation's waterways annually. Dredging this material to maintain navigability is a major item in the Corps' Civil Works budget. To better understand the impact of relocating this dredged material, extensive environmental measurements are made at many placement sites. Seabed drifters (SBD's) are one tool for studying bottom currents at placement sites. SBD's have been widely used in oceanographic, fisheries, and regional sediment tracing studies. Very little is known, however, about how SBD's respond to specific waves and currents. Results of this study should improve the usefulness of SBD's in monitoring open- water disposal sites by quantifying the relative response of sediment and SBD's to the dominant dispersive forces.

RESEARCH: This is the first prototype-scale laboratory study of how SBD's respond to waves and currents. The study focuses on the critical threshold condition at which sand begins to move and examines whether increased weight on the SBD could stall its movement until this threshold is exceeded. Shallow to deep-water waves, alone and with a superimposed current, were studied in combination with different size sands.

SUMMARY: Though often used as an indicator of sediment paths, the size and shape of standard design SBD's are quite different from those of a sand grain. Therefore, SBD's respond differently to currents. Empirical hydrodynamic relationships developed here relate the incipient motion of sand and SBD's under specific conditions. The relationships are complex, and restricted to specific wave frequencies. A range of weights may be necessary to provide correlation between SBD's and sand under changing field conditions.

AVAILABILITY OF REPORT: The report is available through the Interlibrary Loan Service from the U.S. Army Engineer Waterways Experiment Station (WES) Library, telephone number (601) 634-2355, or can be purchased from the National Technical Information Service (NTIS). NTIS report numbers may be requested from WES Librarians.

About the Authors: Dr. Charles K. Sollitt is Director, O. H. Hinsdale Wave Research Laboratory, Oregon State University, Corvallis, Oregon, and Professor, Civil Engineering Department, Ocean Engineering Program. Mr. Edward B. Hands is a research physical scientist in the Coastal Structures and Evaluation Branch, Coastal Engineering Research Center (CERC), U.S. Army Engineer Waterways Experiment Station, Vicksburg, Mississippi. For further information about the Dredging Research Program (DRP), contact Mr. E. Clark McNair, Jr., Manager, DRP, at (601) 634-2070.

December 1994

Dredging Research Program

Technical Report DRP-94-7
December 1994

Correlating Seabed Drifter Weights to Sand Threshold Conditions in Wave and Wave/Current Environments

by Edward B. Hands

U.S. Army Corps of Engineers
Waterways Experiment Station
3909 Halls Ferry Road
Vicksburg, MS 39180-6199

Charles K. Sollitt

O. H. Hinsdale Wave Research Laboratory
Oregon State University
Corvallis, OR 97331

Final report

Approved for public release; distribution is unlimited

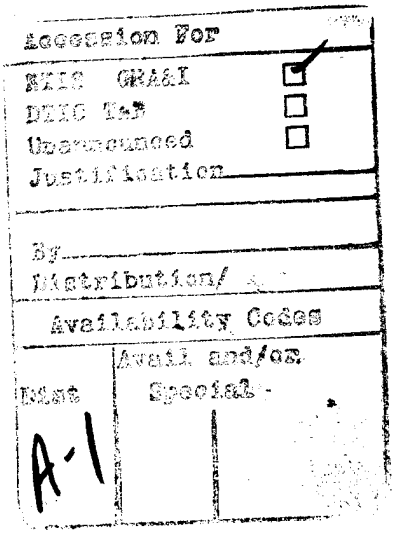

Prepared for U.S. Army Corps of Engineers
Washington, DC 20314-1000
Under Work Unit 32467

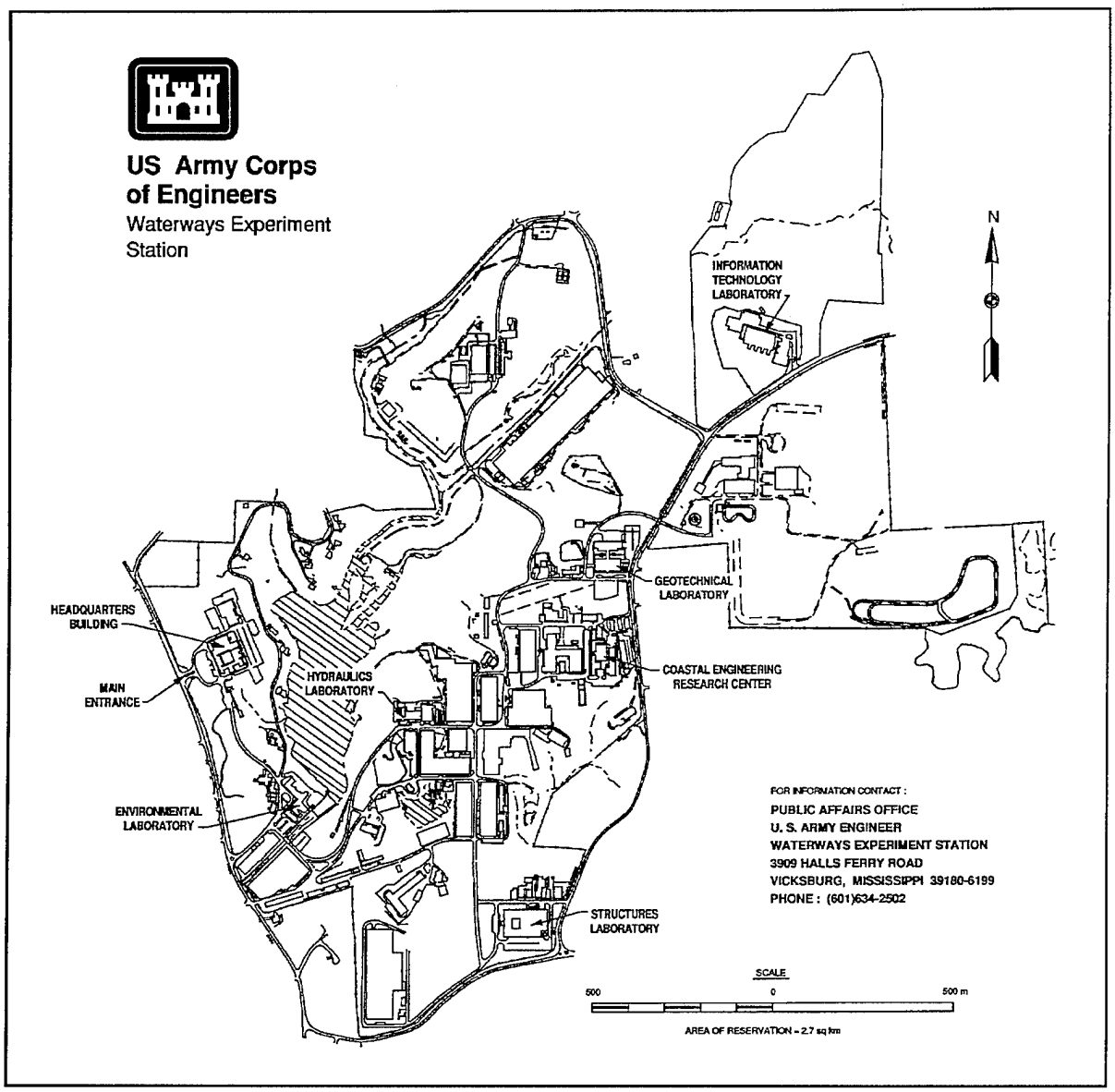

Waterways Experiment Station Cataloging-in-Publication Data

Hands, Edward B.
Correlating seabed drifter weights to sand threshold conditions in wave and wave/current environments / by Edward B. Hands, Charles K. Sollitt ; prepared for U.S. Army Corps of Engineers.
62 p. : ill. ; 28 cm. — (Technical report ; DRP-94-7)
Includes bibliographic references.
1. Ocean circulation — Measurement — Instruments. 2. Ocean bottom. 3. Marine sediments. I. Sollitt, Charles K. II. United States. Army. Corps of Engineers. III. U.S. Army Engineer Waterways Experiment Station. IV. Dredging Research Program. V. Title. VI. Series: Technical report (U.S. Army Engineer Waterways Experiment Station) ; DRP-94-7.
TA7 W34 no.DRP-94-7

Contents

Preface viii

Conversion Factors, Non-SI to SI Units of Measurement x

Summary xi

1—Introduction 1

Problem Statement and Objective 1
Previous Laboratory Response Investigations 2
Present Experimental Design 3
Report Organization 4

2—Theoretical Analysis 5

3—Experimental Apparatus and Procedures 11

Apparatus 11
Procedures 13

4—Results 16

Threshold Wave and Velocity Conditions 16
Dimensionless Drifter Weight Relationships 23

5—Discussion 26

Grain Size and Bed Form Effects on Sediment Threshold Velocities 26
Responses of Seabed Drifters and Effect of Varying Weights 29

6—Examples of Applications 31

Evaluate Threshold Velocity from Figure 5 31
Evaluate Drag-Friction Coefficient Ratio from Figure 10 or 11 32
Solve for Submerged Weight of the SBD from Equation 2 33
Solve Equation 7 for Weight of the Metal Ferrule 33
Alternative Procedures 35
Weights in Water and Air 35

7—Conclusions 36

8—Recommendations for Field Deployments and Lab Studies 38
Field Deployment Recommendations 38
Laboratory Studies Recommendations 38
References 40
Appendix A: Test Conditions and Results A1
Appendix B: Notation B1
SF 298

List of Figures

Figure 1. SBD's moving across seafloor 2
Figure 2. Equilibrium condition between drag force and seabed friction 6
Figure 3. Grain size distribution for Ottawa No. 17 and Ottawa No. 18 12
Figure 4. Reflection coefficient relative to the nondimensional deepwater wave number 17
Figure 5. Near-bed threshold velocity relative to the nondimensional deepwater wave number for "Wave Only" cases 17
Figure 6. Stem-and-leaf display of ratios of different sediment threshold velocities 19
Figure 7. Near-bed threshold velocity compared to SBD fall velocity . . 20
Figure 8. Threshold-fall velocity ratio relative to Keulegan-Carpenter parameter 20
Figure 9. Threshold-fall velocity ratio relative to Reynolds number . . . 21
Figure 10. Drag-friction coefficient ratio relative to Keulegan-Carpenter parameter 21
Figure 11. Drag-friction coefficient ratio relative to Reynolds number . . 22
Figure 12. Inertia-friction coefficient ratio relative to Keulegan-Carpenter parameter 22
Figure 13. Inertia-friction coefficient ratio relative to Reynolds number 23
Figure 14. Bed form effect on threshold velocities 27
Figure 15. Grain size effect on threshold velocities 27

List of Tables

Table 1. Dean's Stream Function Conditions for 11-ft Water Depth 13

Preface

The work described herein was authorized as part of the Dredging Research Program (DRP) by Headquarters, U.S. Army Corps of Engineers (HQUSACE), under Work Unit 32467, "Field Techniques and Data Analysis to Assess Open Water Disposal Deposits." The HQUSACE Chief Advisor for the DRP was Mr. Robert Campbell. Mr. John H. Lockhart was HQUSACE Advisor for DRP Technical Area 1 (TA1), which included Work Unit 32467. The other HQUSACE DRP Technical Monitors were Messrs. Gerald Greener, Barry W. Holliday, M. K. Miles, John Sanda, and David B. Mathis. Mr. E. Clark McNair, Jr., Coastal Engineering Research Center (CERC), U.S. Army Engineer Waterways Experiment Station, was DRP Program Manager. Dr. Lyndell Z. Hales (CERC) was the DRP Assistant Program Manager.

Drs. Nicholas C. Kraus, Senior Scientist, CERC, and Billy H. Johnson were Technical Managers of TA1. Work was conducted under the general supervision of Dr. James R. Houston and Mr. Charles C. Calhoun, Jr., Director and Assistant Director, CERC, respectively. Mr. Edward B. Hands, Engineering Development Division (EDD), CERC, was the contracting officer's representative and the Principal Investigator for Work Unit 32467. Mr. Hands worked under the direct supervision of Mr. Thomas W. Richardson, Chief, EDD; Ms. Joan Pope, Chief, Coastal Structures and Evaluation Branch (CDS); and Dr. Yen-hsi Chu, Engineering Applications Unit.

The wave tank tests were conducted between September 1989 and February 1990 by Dr. Charles K. Sollitt, Director, O. H. Hinsdale Wave Research Laboratory, Oregon State University (OSU); and Messrs. Terence L. Dibble, William H. Hollings, David R. Standley, and John J. Pugh, OSU. Mr. Darryl Bishop determined static properties of SBD's in a series of laboratory tests at CSEB. This report was written by Mr. Hands and Dr. Sollitt based on the contract report (Sollitt 1990). Dr. Ole S. Madsen provided initial recommendations regarding laboratory tests. Ms. Monica A. Chasten and Drs. Yen-hsi Chu, Robert J. Hallermeier, and Nicholas C. Kraus are thanked for technical reviews. Mses Karen Pitchford, systems manager, CDS; Yvette L. McGowan, fellowship student, CDS; and C. Renee Cox, contract student, CDS, assisted in final report preparation.

At the time of publication of this report, COL Bruce K. Howard, EN, was Commander of the Waterways Experiment Station. Dr. Robert W. Whalin was Director.

For further information on this report or on the DRP, please contact Mr. McNair, Program Manager, at (601) 634-2070, or Mr. Hands, Principal Investigator, at (601) 634-2088.

Conversion Factors, Non-SI to SI Units of Measurement

Non-SI units of measurement used in this report can be converted to SI (metric) units as follows:

Multiply	By	To Obtain
degrees (angle)	0.01745329	radians
Fahrenheit degrees	5/9	Celsius degrees or kelvins[1]
feet	0.3048	meters
inches	0.0254	meters
pounds (force)	453.59[2]	grams (mass)
pounds (force) per cubic foot under standard gravity	16.01846	kilograms (mass) per cubic meter
slugs (mass)	14593.9	grams (mass)
square feet	0.09290304	square meters

[1] To obtain Celsius (C) temperature readings from Fahrenheit (F) readings, use the following formula: C = (5/9)(F-32). To obtain Kelvin (K) readings, use K = (5/9)(F-32)+273.15.

[2] To obtain standard metric mass from English force, multiply by:

$$\frac{14593.9 \text{ grams}}{1 \text{ slug}} \quad \frac{1}{32.174 \text{ ft sec}^{-2}} \quad = 453.59 \ \frac{\text{grams}}{\text{pound}}$$

Summary

Seabed drifters (SBD's) have long been used to track bottom currents and infer the transport paths of fine-grained sediment and plankton (e.g. Lee, Bumpus, and Lauzier (1965); Nocross and Stanley (1964)). The laboratory study reported here quantifies, for the first time, how prototype SBD's respond to the combined forces of waves and currents. Also investigated is the possibility of varying the ballast on the SBD stem so that the initial SBD motion occurs at the onset of sediment entrainment for two sand sizes.

Tank tests were conducted using full-size SBD's and prototype waves. Tests in 11-ft (3.4-m) water depths included five monochromatic wave frequencies spanning a range from short, deepwater waves to long, intermediate- to shallow-depth waves. A long wave superimposed on four higher frequencies simulated a mean current superimposed on waves. Two sand sizes were used: one had a median diameter (d_{50}) of 0.21 mm; the other, 0.33 mm.

Acoustic current meters measured instantaneous velocities both near the seabed and at the elevation of the SBD cap where fluid motions exerted the principal drag. During each test, wave amplitudes were increased until sediment motion was initiated on a seasoned bed. Under this incipient motion condition, variously weighted SBD's were introduced to learn which weight would allow the SBD's to pivot on their contact points with the seabed while resisting net translation. This state of equilibrium was defined as the *SBD threshold weighting* corresponding to the particular incipient motion condition being tested. Lightening the SBD's below the equilibrium weighting allowed them to move to the next ripple or beyond during occasional wave passages.

Observed equilibrium conditions were compared to a well-known empirical predictor for initiation of sediment movement from a plane bed. The fall velocities of the variously weighted SBD's were measured and compared to their equilibrium threshold velocities. The measured threshold velocities and submerged weight of the SBD's were combined to examine the effect of flow on drag, friction, and inertial coefficients.

A methodology was derived for using the developed relationships to estimate threshold weightings valid for different sand sizes, waves, and currents. An example shows how to select SBD weightings so that SBD movement begins coincidentally with movement of sand of a specified size. This method

should be valid for a limited, but useful, range of field conditions. Tabulated data and videotapes of incipient motion provide detailed records of experimental results that might be extended by future tests to a wider range of grain sizes and hydrodynamic conditions.

1 Introduction

Problem Statement and Objective

Seabed drifters (SBD's) have long been used to estimate "residual" bottom circulation in slowly varying current fields. Recoveries following releases of large numbers of SBD's have been used, for example, to map the pattern of bottom drift over the inner continental shelf from Newfoundland to Florida (Lee, Bumpus, and Lauzier 1965), from the Columbia River to the Straits of Juan de Fuca (Gross, Morse, and Barnes 1969), and over the Irish Sea (Harvey 1968). In Australia, SBD's were used to map circulation and sediment transport paths in a tide-dominated embayment (Sternberg and Marsden 1979). More recent SBD applications in coastal waters suggest that modifications in deployment and retrieval procedures and changes in ballast weight permit expeditious use of SBD's in active wave environments (Schuldt 1981, Pape and Garvine 1982, Hicks 1986, Hands 1987, Fredette et al. 1990, Resio and Hands 1994). The present study developed relationships between SBD response and wave/current action and investigated the effect of adjusting the ballast weight to attain initial SBD motion coincident with sand movement on the seafloor.

The standard SBD design used in Europe and North America is attributed to P. M. J. Woodhead (Woodhead and Lee 1960). This design is an umbrella-shaped plastic drogue consisting of a 7-in.-diam (18-cm[1]) plastic cap with four 0.7-in. (2-cm) vents and a 22-in. (55-cm) plastic stem (Figure 1). The SBD's used in this study were about 3.0 grams buoyant. Depending on the specific gravity of the plastics composing the SBD's, buoyancies have ranged from 2.8 to 6.5 grams in previous studies conducted by the U.S. Army Engineer Waterways Experiment Station (WES). The buoyancy is overcome by crimping a metal ferrule near the bottom of the stem. Further increasing the ferrule weight should create a resistance to the drag-induced motion as investigated here.

[1] Original units of measurement are retained as the primary expression. Conversion factors for SI units are presented on page x of this report.

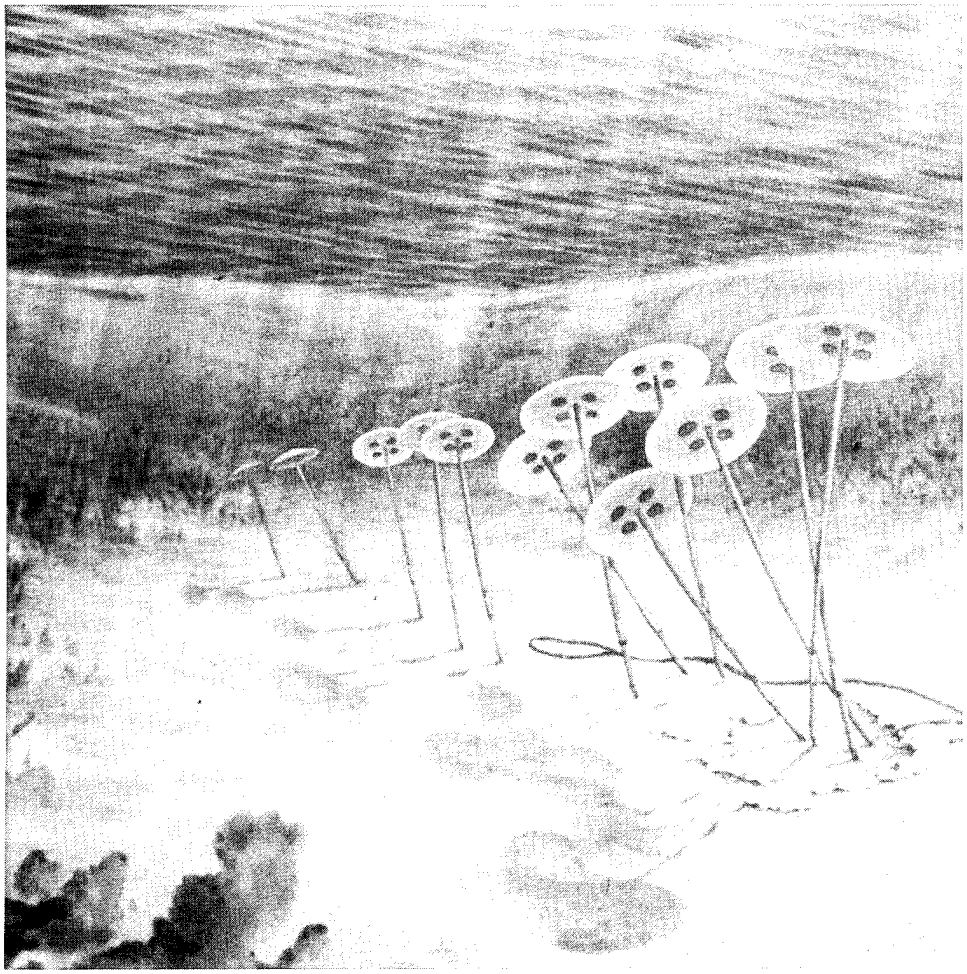

Figure 1. SBD's moving across seafloor

The responses of differently weighted SBD's to large-scale laboratory waves sufficient to induce motion of sands with a diameter (d_{50}) of 0.21 and 0.33 mm were studied. "Wave Only" and "Wave with Current" threshold conditions covered a range of Dean's stream functions from 4 to 8 (Dean 1974).

Previous Laboratory Response Investigations

Hundreds of thousands of SBD's released around the world have adhered to the standard design dimensions introduced in 1960. These rugged, inexpensive plastic drogues quickly replaced heavily weighted drift bottles that had been released in oceanographic studies at least since the turn of the century. Quantification of the hydrodynamic response of SBD's has, however, received little study. This deficiency may be because field-documented trajectories, revealed by SBD's, reflected the summation of many time-varying displacements over long intervals; and objectives were often to get only some initial insight into

large-scale, general circulation patterns. It is inherent in such applications that many potential influences, including the following, will be poorly known: the actual SBD path, the time between the arrival of the SBD at its recovery site and its recovery, the possibility that snagging in kelp or on some other bottom obstruction biased the elapsed times or the chances of recovery. Additional complications include the effects of winds, waves, eddies, and other currents varying spatially and temporally during the SBD journey.

Factors affecting the percent and accuracy of recovery information were specifically investigated by Riley and Ramster (1972) and by Bartolini and Pranzini (1977) using, among other techniques, "bogus SBD plantings" at known beach locations. Some of the other uncertainties mentioned above are reduced or eliminated in nearshore deployments or by attaching a sonic transmitter to the SBD's (Folger 1971, Hands 1987). New techniques improve interpretation and quantify components of mean SBD displacement and random dispersion (Resio and Hands 1994).

Woodhead and Lee (1960) selected the present SBD design based on flume experiments at Liverpool University. Laboratory studies seem well-suited to quantifying how SBD's respond to specific hydrodynamic forces, but only two tests are known. Mr. D. J. Ellett correlated the speeds of SBD's with water flowing at various rates in 2.5- and 5-m (8- and 16-ft) flumes (Phillips 1970). The reported regression equation showed SBD speed increasing linearly with the steady flow. Accordingly, movement began at a threshold near 4 cm/sec and had reached 80 percent of the fluid speed when the unidirectional flow was about 32 cm/sec (1 ft/sec).

In the second study, Collins and Barrie (1979) superimposed oscillations on a steady current in a 4-m-long by 0.3-m-deep (13-ft by 1-ft) recirculating flume. The shallow flume depth required shortening the SBD stem from 55 to 12 cm. By varying the frequency of an oscillating carriage over the flume, Collins and Barrie showed a period-dependent reduction in the threshold speed below the value Phillips had reported.

Present Experimental Design

For the work reported herein, the stem ballast was modified on full-scale Woodhead SBD's until incipient SBD motion was observed coincident with incipient sediment motion in a sequence of experimental runs covering a range of wave, current, relative depth, and sediment conditions. Various instruments recorded wave height and period, water velocities at different elevations above the bed, the profiles of incident and reflected waves, and the simultaneous responses of the sand grains and SBD's.

Report Organization

Chapter 2 describes theoretical bases for the equilibrium conditions. Test procedures and data collection are detailed in Chapter 3. Relative drag and inertia coefficients for SBD's are evaluated and related to the Reynolds numbers and the Keulegan-Carpenter (K-C) parameters for each test in Chapter 4. A general predictive procedure is derived for assessing threshold SBD weightings in Chapter 5 and an example problem is worked in Chapter 6. Appendix A tabulates data on test conditions and results and Appendix B is a notation of symbols and abbreviations used in this report.

2 Theoretical Analysis

For fairly steady hydrodynamic conditions, the ferrule weight of an SBD was adjusted so that drag between the fluid and the SBD balances frictional resistance between the SBD and the seabed. Reduction in ferrule weight below the threshold weighting would have permitted SBD motion across the seabed.

Before testing SBD response in another run (a different wave/current/sediment condition), the tank was seasoned to establish a new ripple pattern. It was reasoned that, in Nature, waves exceeding the sediment threshold condition quickly establish quasi-equilibrium sand ripple patterns so that most near-bottom transport occurs over ripples. Furthermore, pre-existing ripples are more likely than a perfectly smooth seabed as the initial nearshore bed state, even when velocities first increase above the sediment threshold value.

The operational definition of incipient motion allowed the SBD to move to and fro between adjacent ripple crests, but not move over them during observation periods of about 40 wave passages. Incipient sediment motion criteria required that no erosion occurred along the crest of the ripples. At bed irregularities and where the stem of an SBD pivoted against a ripple crest, a few grains would be dislodged during occasional peak velocities. The bed form patterns, however, remained stationary under the equilibrium test conditions.

Equilibrium between the drag force on the SBD and friction where the stem contacted the seabed, at a velocity corresponding to the threshold condition, is depicted in Figure 2. A simple representation of this equilibrium is

$$\mu W = F_D = \rho\, C_D\, A \frac{U^2}{2} \qquad (1)$$

where

μ = friction coefficient between SBD and seabed [dimensionless]

W = submerged weight of SBD [mass length/(time)^2]

F_D = drag force on SBD [mass length/(time)^2]

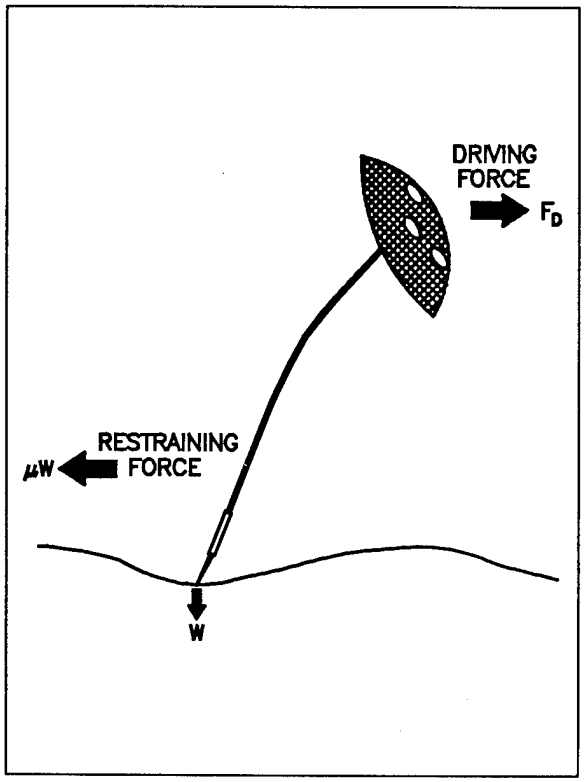

Figure 2. Equilibrium condition between drag force and seabed friction

ρ = density of water [mass/(length)^3]

C_D = drag coefficient [dimensionless]

A = projected area of SBD (cap area) [length^2]

U = sediment threshold velocity amplitude [length/time]

Knowing C_D/μ, one could solve for the required ferrule weight that caused the SBD to mimic the threshold characteristics for the sediment. To find C_D/μ, Equation 1 is inverted to yield

$$\frac{C_D}{\mu} = \frac{2W}{\rho A U^2} \qquad (2)$$

Here, U could be experimentally observed as the threshold velocity for a particular wave and sediment condition, and the submerged weight W would include the minimum weight ferrule required to keep the SBD from translating.

The drag coefficient C_D is known to depend on real fluid properties, as expressed in the Reynolds number R_e

$$R_e = \frac{UD}{\nu} \qquad (3)$$

where

D = characteristic length (cap diameter) [length]

ν = kinematic viscosity of water [(length)^2/time]

The drag coefficient also depends on the size of the object compared to the trajectory of the wave-induced particle motion, as expressed in the Keulegan-Carpenter parameter (Sarpkaya and Isaacson 1981, Chakrabarti 1991):

$$K\text{-}C = \frac{UT}{D} \tag{4}$$

where

T = wave period [time]

The cap diameter of 7.0 in. was used as the characteristic length to evaluate both of these parameters. A kinematic viscosity value of 1.41×10^{-5} ft^2/sec was used for the 50 °F (10 °C) water in this experiment. Because C_D/μ was expected to vary with changes in wave/sediment conditions, its variability was investigated relative to the Reynolds number and the Keulegan-Carpenter parameter.

Waves exert inertial as well as drag forces. The inertial force is proportional to fluid acceleration and, for small-amplitude waves, is 90 deg out of phase with the drag force. This causes the inertial force to be maximum when the drag force is zero and vice versa.

The inertial force may be written as

$$F_I = \rho C_I V a \tag{5}$$

where

F_I = inertial force [mass length/(time)^2]

C_I = inertial coefficient, dimensionless

V = volume of SBD [length^3]

a = amplitude of unsteady fluid acceleration = $\frac{2\pi U}{T}$ [length/(time)^2]

The volume of the assembled drifter V was determined by averaging the loss of weight due to immersion of 30 SBD's in a fluid of known density.

When inertial forces dominate, the equilibrium equivalent to Equation 1 is

$$\mu W = F_I = \rho C_I V a = \rho C_I V \frac{2\pi}{T} U \tag{6}$$

The submerged weight of the assembled SBD W includes the weight of the metal ferrule W_f less the net buoyancy of the remaining plastic parts $-W_d$, which is about 0.007 lb (or equivalent to about 3-gram mass). Thus,

$$W = W_f + W_d \approx W_f + (-0.007)\,lb \tag{7}$$

The drag-to-friction coefficient ratio expressed in Equation 2 was evaluated experimentally by measuring the threshold velocity amplitude U for a particular wave period T and increasing the ferrule weight W_f until net translation of the SBD ceased. The resulting drag-to-friction coefficient was then examined as a function of the Reynolds number and the Keulegan-Carpenter parameter. Similar analysis was done with respect to the inertial-to-friction coefficient ratio.

Typically, drag and inertial coefficients are assumed to be time independent (Morison et al. 1950) and combined to yield a time-varying total force. One component of the total force varies as sin $2\pi t/T$ and the other as cos $2\pi t/T|\cos 2\pi t/T|$ because the fluid velocity varies as cos $2\pi t/T$.

The total time-dependent, wave-induced, longitudinal force F acting on a stationary body is thus

$$F = F_D + F_I \tag{8}$$

$$F = \rho C_D A \frac{U^2}{2} \cos\frac{2\pi t}{T}\left|\cos\frac{2\pi t}{T}\right| + \rho C_I V \frac{2\pi U}{T}\sin\frac{2\pi t}{T} \tag{9}$$

The forces may be nondimensionalized with respect to the amplitude of the drag force according to

$$\frac{F}{\rho C_D A \frac{U^2}{2}} = \cos\frac{2\pi t}{T}\left|\cos\frac{2\pi t}{T}\right| + \frac{C_I V 4\pi}{C_D A U T}\sin\frac{2\pi t}{T} \tag{10}$$

Let the dimensionless ratio in the second component be represented by the symbol I

$$I = \frac{C_I V 4\pi}{C_D A U T} \tag{11}$$

If I is much less than unity, drag forces dominate the wave load on the body and inertial forces may be ignored. The relationship among independent variables in Equation 11 shows that long-period waves and objects of small volume per unit area involve smaller inertial forces. When I is less than 1/10, the flow is drag-dominated and the SBD response is insensitive to the unsteady flow effects, so the total force is equivalent to that induced by a steady current of equal velocity magnitude. Superimposing a long drag-dominated wave on short waves thus provided an additive maximum drag force similar to that provided by adding a steady current on top of wave oscillations.

To estimate I for sand particles, a spherical grain shape is assumed so that

$$\frac{V}{A} = \frac{(4\pi/3)(d^3/8)}{\pi(d^2/4)} = \frac{2d}{3} \tag{12}$$

where

d = diameter of a sphere [length]

The inertial and drag coefficient values for a sphere are

$C_I = 1.5$

$C_D = 0.5$

The 10-sec wave used to simulate a current in this study produced threshold velocities of approximately 6 in./sec (150 mm/sec) with a d_{50} of 0.3 mm. Accordingly, the inertia ratio in Equation 11 becomes

$$I = \frac{C_I}{C_D}\frac{V}{A}\frac{4\pi}{UT} = \frac{1.5}{0.5}\frac{2\ (0.3mm)}{3}\frac{4\pi}{150mm/sec\ (10sec)}$$

$I \sim 1/200$

This low value of I shows that wave-induced inertial forces on the surface sediment particles were approximately 0.5 percent of the drag forces for 10-sec wave periods.

A similar argument can be made for the relative importance of drag and inertial forces on the SBD. Using average values of weight and specific gravity determined for a large number of representative SBD's at the WES Coastal Engineering Research Center (CERC) resulted in the following:

$$\frac{V}{A} = \frac{40.4cm^3}{109cm^2}$$

For the same hydrodynamic conditions used in the evaluation of the sand grain, Equation 11 becomes

$$I = \frac{C_I}{C_D}\frac{V}{A}\frac{4\pi}{UT} = \frac{C_I}{C_D}\ 3.7mm\ \frac{4\pi}{150mm/sec\ (10sec)}$$

$$I < \frac{C_I}{C_d}\frac{1}{30}$$

Though the drag and inertial coefficients for such a complex shape as the SBD are unknown, they are presumably of the same order of magnitude. Thus the ratio of forces is smaller than 1 for SBD's.

Low values of I show that the 10-sec wave exerts a drag-dominated force approaching that of a steady current. Superimposing short waves on this 10-sec wave thus produces dynamically similar behavior to superimposing short waves on a mean current.

The sand grain threshold velocity is found experimentally by observing the onset of erosion from the crest of an equilibrium ripple pattern. The resulting values were compared with predicted values suggested by Komar and Miller (1973) and summarized here as

$$\frac{\rho U^2}{(\rho_d - \rho) g d_{50}} = 0.21 \left(\frac{B}{d_{50}} \right)^{1/2} \tag{13}$$

where

d_{50} = diameter of sediment grains [length]

B = orbital diameter of wave motion at seabed [length]

The wave-induced velocity U and orbital diam B are related via linear wave theory as

$$U = \frac{\pi B}{T} = \frac{\pi H}{T \sinh(2\pi d/L)} \tag{14}$$

where

H = wave height [length]

h = water depth [length]

L = wave length [length]

The wave length L is solved from the linear wave theory dispersion relationship as a function of h and the wave period T.

3 Experimental Apparatus and Procedures

Apparatus

Viscous scale effects distort drag forces in small model facilities. Oregon State University's large, two-dimensional wave channel was used to study full-scale SBD's at near-prototype Reynolds numbers. The wave channel is 342 ft long, 12 ft wide, and 15 ft deep. This facility can generate monochromatic and random waves up to 5 ft high in a water depth of 11.5 ft. The useful period of the flap-type hydraulic wave generator ranges from 1 to 10 sec.

A 1:12 slope beach, fabricated from 12-ft-square by 6-in.-thick concrete panels, was placed at the end of the wave channel opposite the wave generator. The bottom two panels of the beach were sloped at 1:6.

A test section of granular seabed material was placed 48 ft from the toe of the beach and 101 ft from the wave board. Sand seabed samples were prepared in parallel pallets, 12 ft long by 6 ft wide by 6 in. thick, placed on the bottom of the wave channel. Concrete beach panels were placed in front of and behind the test section to provide continuity in depth. An overall water depth of 11.5 ft was used for all tests, providing an 11-ft depth over the test section.

Sand was obtained commercially. Ottawa sand was chosen because it is rounded like natural seabed material and has been hydraulically washed to remove the fines. Ottawa No. 17 sand was used as the coarse material with a specified manufacturer's d_{50} of 0.23 mm. Size analysis at Oregon State University showed the d_{50} was 0.33 mm. Ottawa No. 80 sand was used as the fine material with a specified manufacturer's d_{50} of 0.16 mm. Size analysis at Oregon State University showed the d_{50} was 0.21 mm. Measured grain size distributions are presented in Figure 3. The key in Figure 3 identifies the manufacturer's specified grain size as "Specs" and the measured grain size as "Analysis."

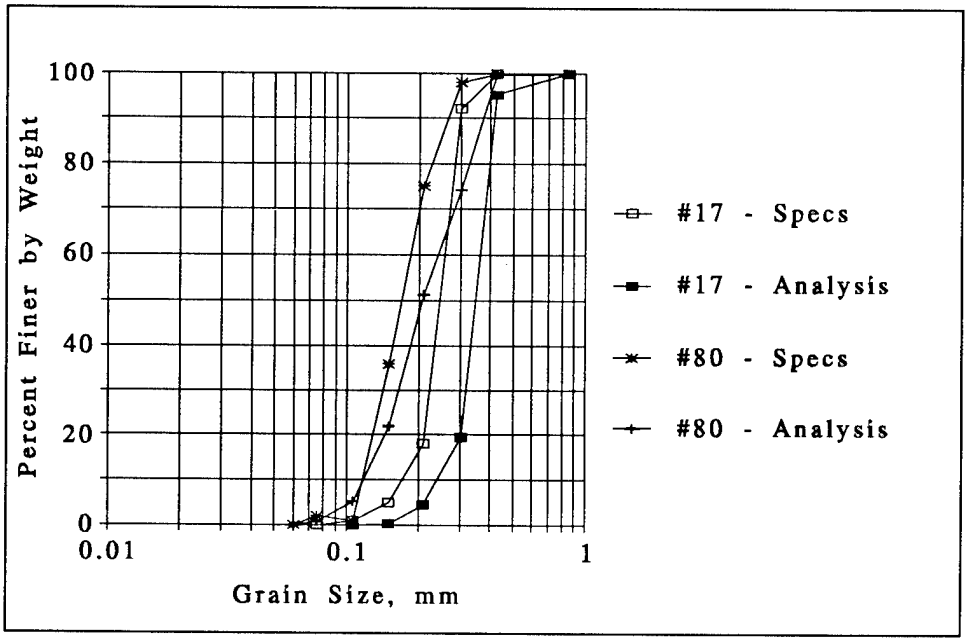

Figure 3. Grain size distribution for Ottawa No. 17 and Ottawa No. 18

According to the Uniform Soil Classification System, both sands are classified as fine-grained. Nevertheless, to distinguish their relative sizes in the narrative and figures of this report, the Ottawa No. 17 sand will be called "Coarse" and the Ottawa No. 80 sand will be called "Fine."

The materials were placed under water to minimize air entrainment and screeded to a uniform depth of 6 in. Test materials were placed in a 6-ft-wide section on the near (east) side of the wave channel. A coarse material with a d_{50} of approximately 1 mm was placed on the far side of the wave channel to provide a continuous depth across the seabed.

Underwater color television cameras were secured to the east wall of the wave channel to provide a visual record of ripple formation and sand erosion. One camera was equipped with a telephoto lens and the other a wide-angle lens. The cameras were SeaCams, model SC-2000. A 2-ft-square black plate with a 3-in. grid etched on the surface was placed vertically in the center of the wave channel on the seabed. The plate served as a background and reference plane for the video documentation. Monitors and VCR's for the cameras were located in an elevated control room, 14 ft above and 36 ft northeast of the test section.

Seabed velocity measurements were obtained with Neil Brown acoustic current meters secured to the walls of the wave channel at the center of the test section. The current meter located on the east wall sampled velocities 3 in. above the seabed. The current meter located on the west wall sampled velocities 16.5 in. above the seabed, at the approximate height of the SBD cap. Velocities were recorded on an oscillograph in the elevated control room.

Measured threshold velocities are presented and compared to the theory of Komar and Miller (1973) in Chapter 4, "Results."

Water surface elevations were measured with two Sonic Systems acoustic profilers. A fixed profiler was placed at the center of the test section, above the current meters. A mobile profiler was placed on a carriage between the wave generator and test section. Wave reflection coefficients were resolved using two methods. First, the wave envelope was profiled with a moving gauge and the reflection coefficient calculated as the difference between the envelope maxima and minima divided by the sum. Second, the Goda method was used requiring signals from two fixed gauges at a known spacing (Goda and Suzuki 1976). The results of both methods are presented and compared in Chapter 4, "Results."

Procedures

Five monochromatic wave conditions were selected to span the range from short deepwater waves (h/L + 1/2) to relatively long intermediate- to shallow-depth waves. These wave conditions correspond to Dean's Stream Function cases 4 - 8 (Dean 1974). The resulting wave periods and lengths for the 11-ft water depth over the test section are presented in Table 1. Dean's case 3 was not examined because the wave length would exceed the distance between the wave board and mid-depth on the beach resulting in a complex, nonperiodic wave form and velocity in the channel.

Table 1
Dean's Stream Function Conditions for 11-ft Water Depth

Case	h/L_0	h/L	*T*,sec	*L*,ft
8-A	0.50	0.50	2.07	22.3
7-A	0.20	0.22	3.28	49.5
6-A	0.10	0.14	4.64	79.0
5-A	0.05	0.09	6.56	119.0
4-A	0.02	0.06	10.37	197.2
3-A	0.01	0.04	14.66	285.5

The long wave (Dean's case 4) simulated a current at the equilibrium conditions as already justified in Chapter 2, "Theoretical Analysis." The wave amplitude of the long wave was adjusted to provide approximately one-half of the sediment threshold velocity indicated for Dean's case 4. Graphical results for this condition are called "Wave and Current" in the text of this document and the keys to the illustrations. Single frequency wave conditions are called "Wave Only."

A minimum of 2 hr of wave excitation seasoned the tank before each new test. Seasoning was done with a wave height approximately 50 percent greater than that needed for sediment threshold conditions. Seasoning thus established baseline equilibrium seabed ripple patterns. The waves were then stopped. After all oscillation ceased, the instrumentation and tank were powered up to generate waves at the period used in the seasoning condition, but with a wave height one half the threshold wave height (one third that used in the seasoning). The wave height was then gradually increased until incipient motion was observed at the crest of the ripples in the cameras's fields of view. This defined the operational threshold velocity and the wave height and period to be used in the following runs.

Again, the waves were stopped until motion in the channel ceased. Then the threshold wave condition was reestablished, and kinematic measurements were made including:

a. Two velocity measurements at 3 in. and 16.5 in. above the seabed.

b. Simultaneous wave profiles at fixed points above the center line of the test section and a known distance toward the wave generator.

c. A moving profile of the combined incident and reflected wave envelope between the test section and wave generator.

A six-channel oscillograph recorded results from each run for subsequent manual interpretation. Only the "Wave and Current" (two-frequency) wave profiles were recorded digitally for computer interpretation.

Each run was repeated once more for video documentation and SBD weight tests. Modifications were based on estimates from the previous run. Three SBD's were used; one with the estimated adjustment, one heavier, and one lighter. All SBD's were the same as used in field work except they did not have postal return cards attached as is often done in field studies.

The underwater television cameras recorded the SBD motion. Any SBD that experienced translation beyond a ripple dimension was under-weighted for that threshold condition. The weight was increased until a weight was found that permitted only a short excursion between adjacent ripple crests. The approximately 10 percent heavier weighted SBD was confined within a single ripple trough. This heavier weight was recorded as the *equilibrium weighting* for the flow conditions and sand being tested.

Unreported CERC field measurements had shown substantial reduction in the SBD speeds when the stems were shortened, as required by Collins and Barrie (1979) in their scaled down flume study. No such modifications in stem length were required to establish threshold weightings in this series of tank tests.

In a few cases, however, it was necessary to use a thicker than normal brass ferrule. Increasing the length of the standard thin-walled ferrule (9/32-in. ID and 3/8-in. OD) beyond 3 in. raises the center of gravity of the SBD's so they do not readily right themselves. To avoid possibly altering the equilibrium conditions, ferrules weighing more than 15 grams were cut from 3/8-in.-ID and 1/2-in.-OD material. All ferrules were crimped to provide approximately 1/2 in. of exposed plastic stem below the weight.

Fall velocities for the variously weighted SBD's were measured by dropping each SBD in still water. Observations through an underwater window established the vertical displacement as a function of time. Path lengths of 2 ft or less were observed using a hand-held level to avoid parallax errors.

The first five wave cases listed in Table A1 were run as single frequency, "Wave Only" conditions. These were followed by four "Wave with Current" simulations. Period conditions for these nine waves were then repeated for "Fine Sand" conditions. "Coarse Sand" was investigated first and corresponds to runs 1-9 in Table A1. The sand was replaced in the section and the experimental sequence was repeated (runs 10-18). These "Fine Sand" results are reported as runs 10-18 in Table A1.

4 Results

Experimental results include threshold wave and velocity conditions for the seasoned sand beds and SBD threshold weighting conditions. The order of discussion and data tables are divided accordingly.

Threshold Wave and Velocity Conditions

Measurements of equilibrium wave height, length, and period are summarized in Table A1, along with dependent wave parameters calculated for these low-amplitude waves by linear theory. Wave reflection coefficients were calculated using both the wave envelope and Goda's expressions. Definitions for all symbols are compiled in Appendix B, "Notation."

Figure 4 summarizes the reflection coefficient as a function of the deepwater wave number. The deepwater wave number is the classical nondimensional expression for water depth relative to the wave period ($4\pi^2 h/gT^2$). This parameter is proportional to the water depth divided by the deepwater wave length ($2\pi h/L_o$). As the wave number increases, the reflection coefficients tend to decrease. This observation is consistent with accepted theory, in which shorter waves are more effectively attenuated by breaking on an inclined beach. The long waves experienced reflections of approximately 20 percent, whereas the short waves experienced reflections of approximately 5 percent. The Goda method indicates one anomalous point at a wave number of 2. Except for the case of the longest wave length, typical reflection coefficients in these tests were 12 percent or less.

Measured and predicted threshold velocities are presented as a function of nondimensional deepwater wave number in Figure 5. These data are tabulated as *utb* and *up*, respectively, in Table A2. Measurements of *utb* were made 3 in. above the seabed and represent near-bed velocity amplitude. The predicted velocities *up* are those evaluated using Equation 13, which refers to the peak speed just above the wave boundary layer.

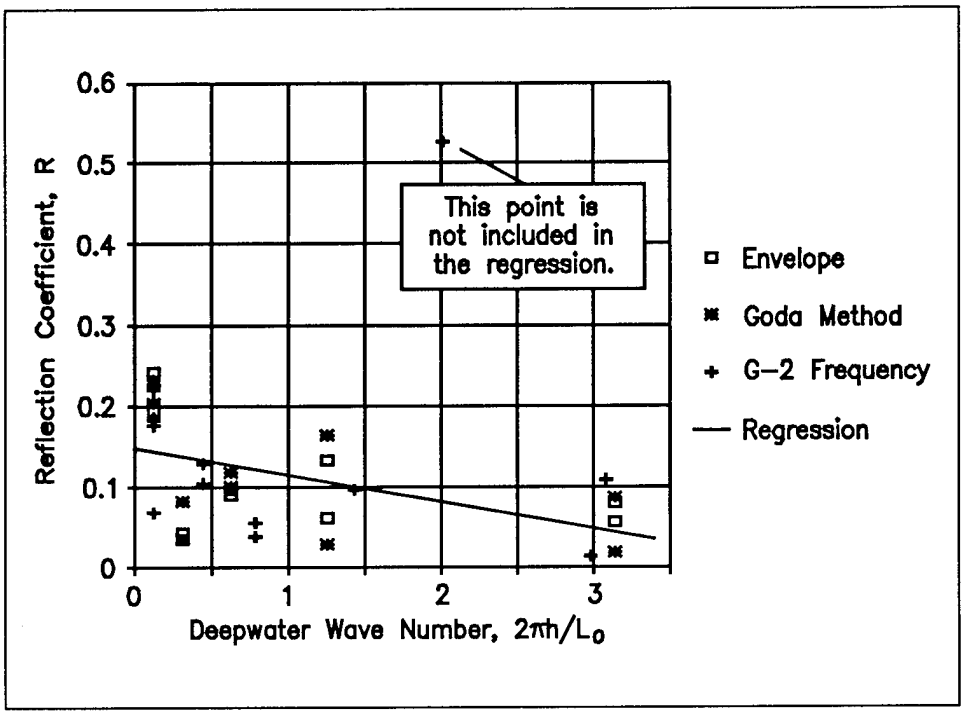

Figure 4. Reflection coefficient relative to the nondimensional deepwater wave number

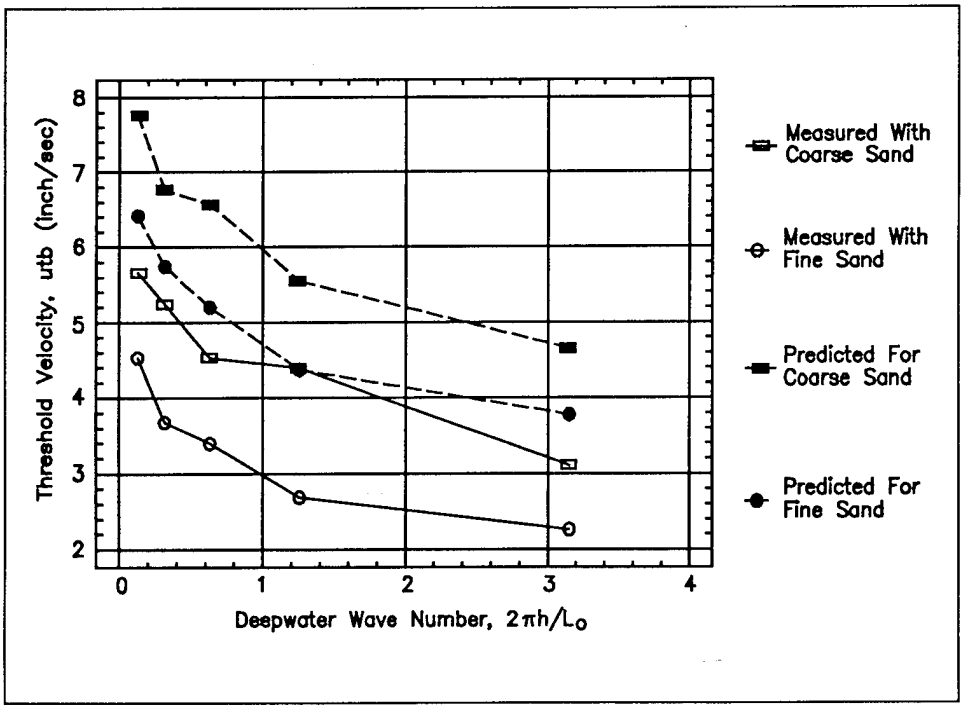

Figure 5. Near-bed threshold velocity relative to the nondimensional deepwater wave number for "Wave Only" cases

Figure 5 shows that the measured threshold velocities for the coarse sand ("Measured with Coarse Sand") exceed those for the fine sand ("Measured with Fine Sand") by about 50 percent. In both cases, the velocities decrease smoothly as wave number increases, showing that longer wave periods require higher near-bed velocities to mobilize sediment. This behavior is supported by most of the 18 empirical equations reviewed by Sleath (1984) and by the more recent extensive measurements by King (1991).

Figure 5 also shows, however, that the predictions exceeded the threshold velocities measured. Komar and Miller's prediction theory applies to smooth beds whereas measurements in this study were over rippled beds. Thus, lower threshold velocities in the present study are consistent with earlier observations that a flat bed is the most stable bed state. Ripples induce turbulence, reduce grain stability, and thus lower the velocities required to entrain sediment. Though the ratios of threshold velocities for "Coarse" versus "Fine" conditions and the ratios for measurements versus theory both varied between about 1.2 and 1.7, the typical ratios (mean, median, and mode of the ratios) were close to 1.5, as seen in Figure 6. Thus, sediment motion initiation on a flat bed seems to occur at a shear velocity about 50 percent greater than on a rippled bed with equivalent grain sizes. Note the change from "Coarse" to "Fine Sand" had a similar effect.

The measurements of threshold velocities under the combined "Waves and Currents" could not be compared to predictions, because the predicted values are for purely oscillatory flow.

Figures 7 through 13 separate the SBD force coefficients by grain size and "Wave Only" or "Wave and Current" thresholds. A key in each figure identifies the following combinations:

a. "Wave Only with Coarse Sand": Refers to the equilibrium condition (simultaneous incipient motion for SBD's and sand) with the relatively coarse Ottawa No. 17 sand and various single-frequency waves.

b. "Wave and Current with Coarse Sand": Refers to the equilibrium condition with relatively coarse Ottawa No. 17 sand and a low-frequency wave (a 10.4-sec wave simulating a steady current) superimposed on various high-frequency waves.

c. "Wave Only with Fine Sand": Refers to the equilibrium with relatively fine Ottawa No. 80 sand and various single-frequency waves.

d. "Wave and Current with Fine Sand": Refers to the equilibrium with relatively fine Ottawa No. 80 sand and various high-/low-frequency wave combinations.

Open plot symbols refer to "Wave Only." Closed symbols represent "Wave and Current" combinations. The boxes are for "Coarse Sand" threshold conditions; the circles represent "Fine Sand" threshold conditions.

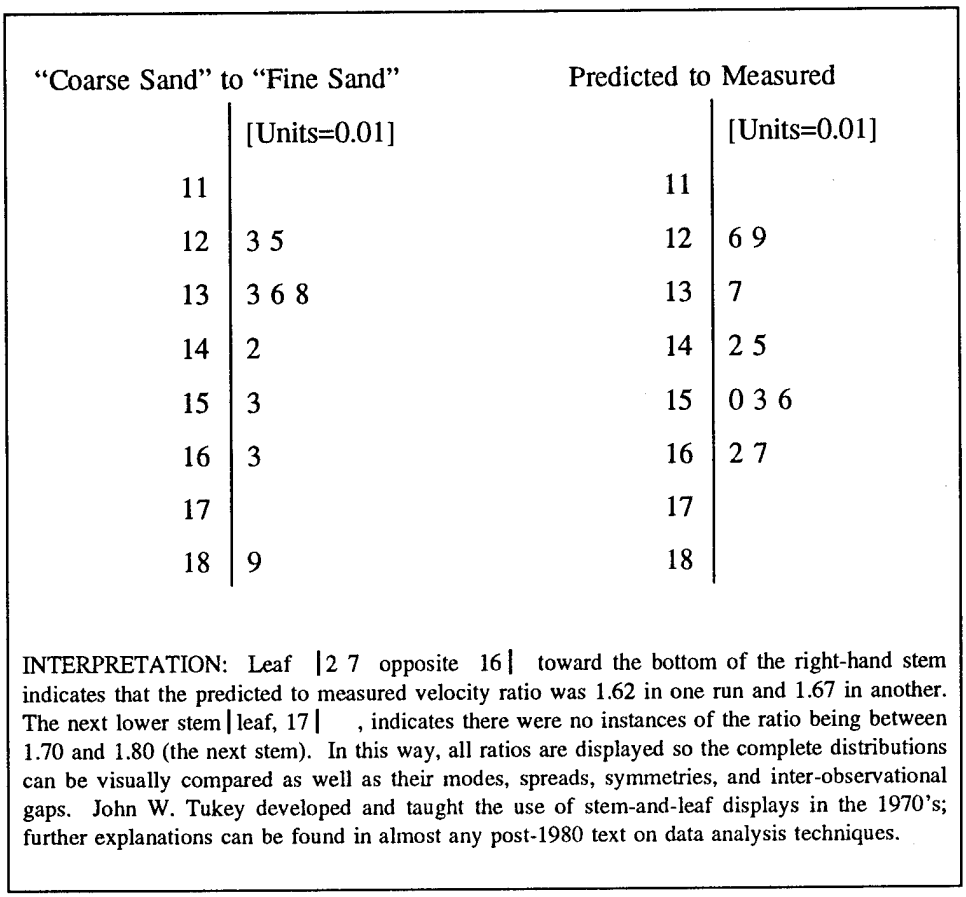

Figure 6. Stem-and-leaf display of ratios of different sediment threshold velocities

Fall velocities were evaluated for the variously weighted SBD's. The resulting relationship between threshold and fall velocities (*utb* and *uf*) can be examined in Figure 7. One might expect that faster threshold velocities would correspond to heavier stem weights that yield faster fall velocities. On the contrary, the results show a decrease in fall speed corresponding to an increase in threshold speed. The effect is particularly evident in the "Wave Only with Coarse Sand" condition. With the superposition of a current this dependency becomes markedly subdued. With the finer sand, not only is the correlation subdued, but the superposition of a current induces very little change in the force coefficients and therefore the equilibrium SBD weighting. There is no simple relationship between threshold velocity and the equilibrium weighting. The counter-intuitive correlation for "Wave Only Coarse Sand" will be referred to again in Chapter 5, "Discussion." To better resolve the effects of grain size, wave period, and a superimposed current on threshold velocities and SBD weights, the standard nondimensional parameterizations for fluid forces are examined in the next series of figures (Figures 8-13).

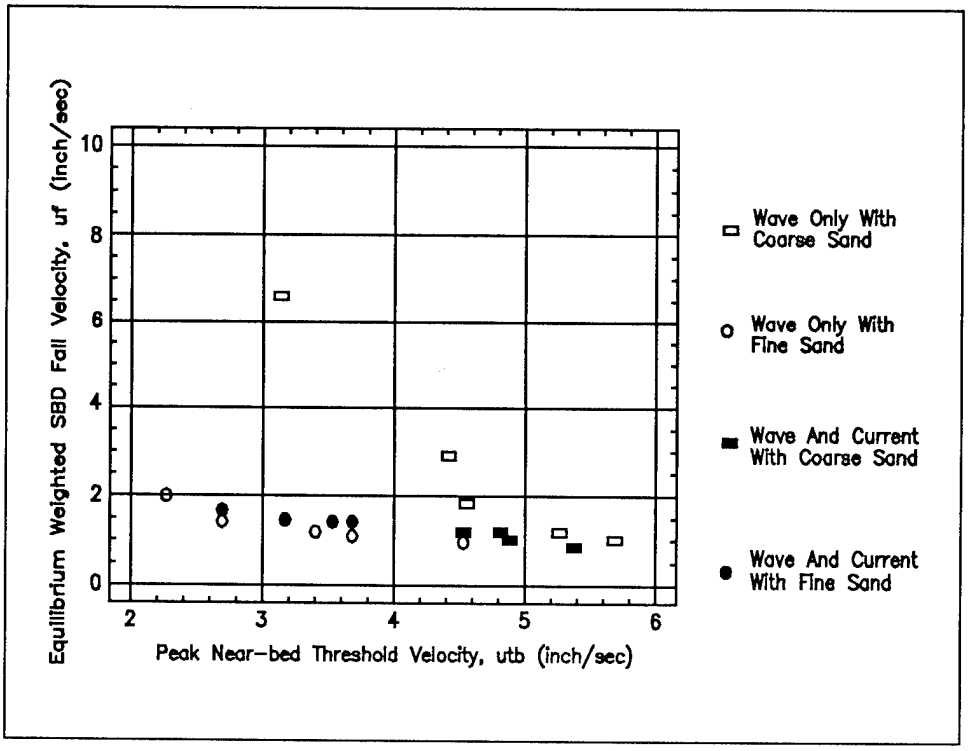

Figure 7. Near-bed threshold velocity compared to SBD fall velocity

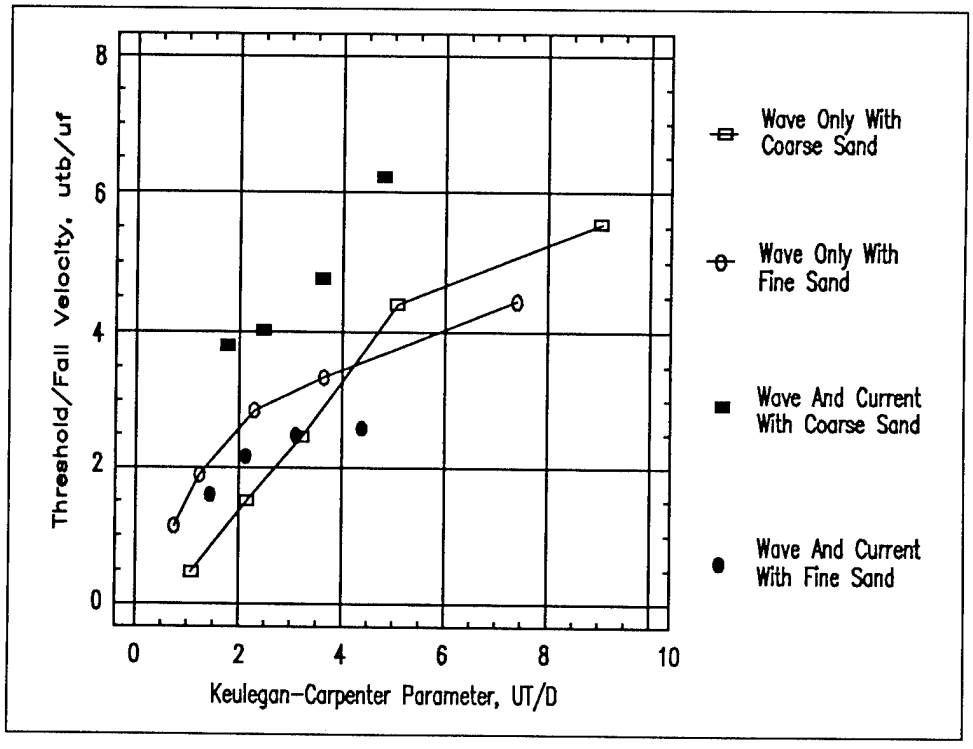

Figure 8. Threshold-fall velocity ratio relative to Keulegan-Carpenter parameter

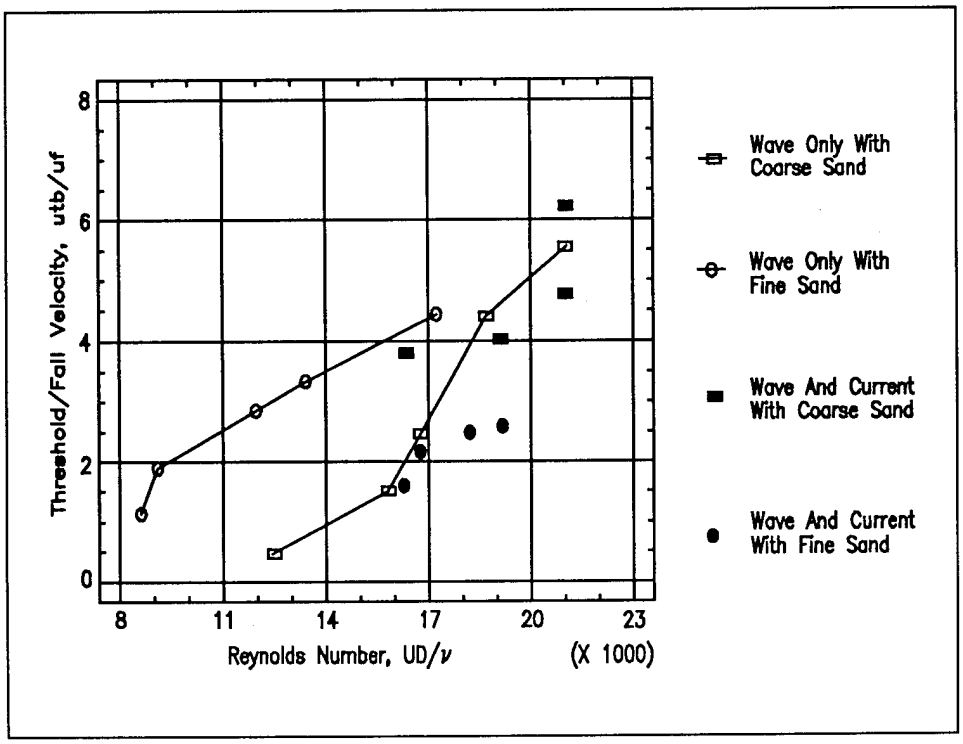

Figure 9. Threshold-fall velocity ratio relative to Reynolds number

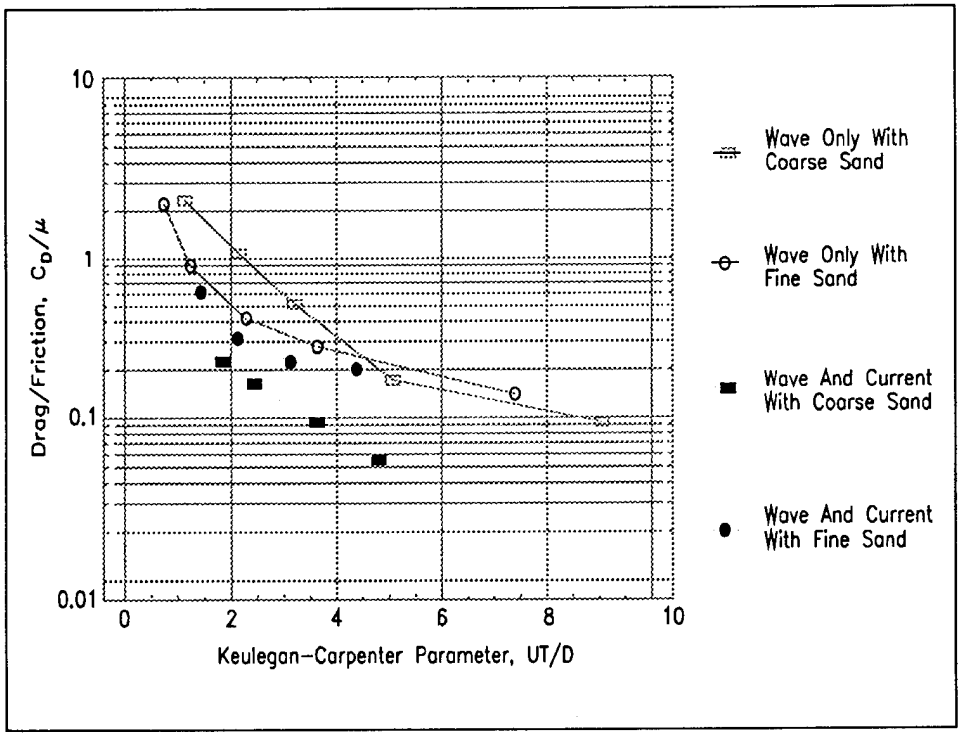

Figure 10. Drag-friction coefficient ratio relative to Keulegan-Carpenter parameter

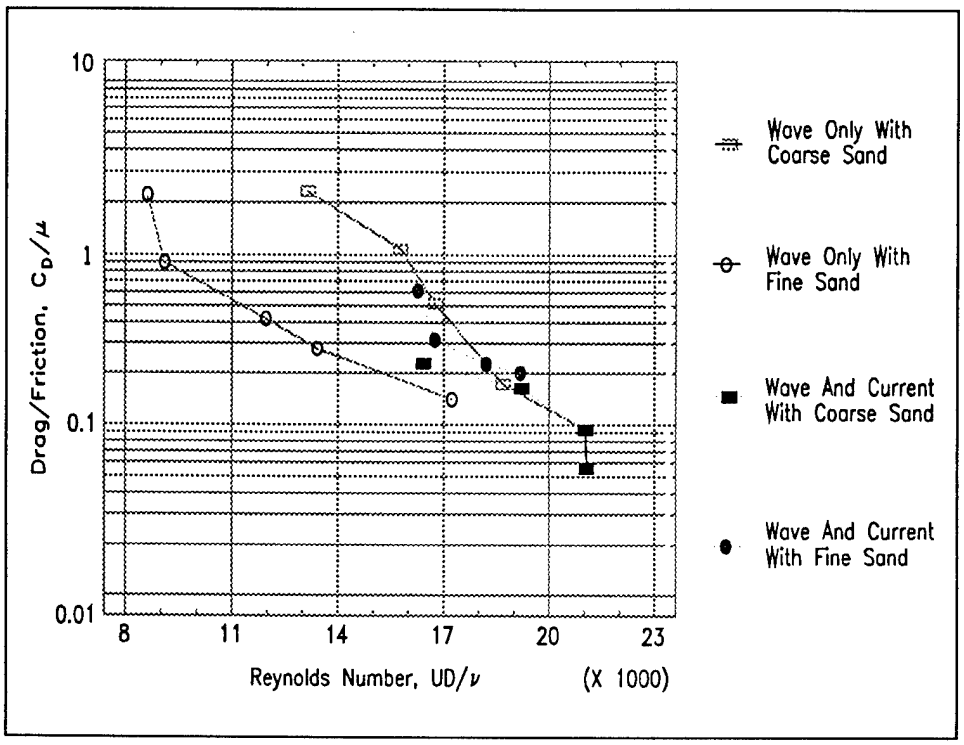

Figure 11. Drag-friction coefficient ratio relative to Reynolds number

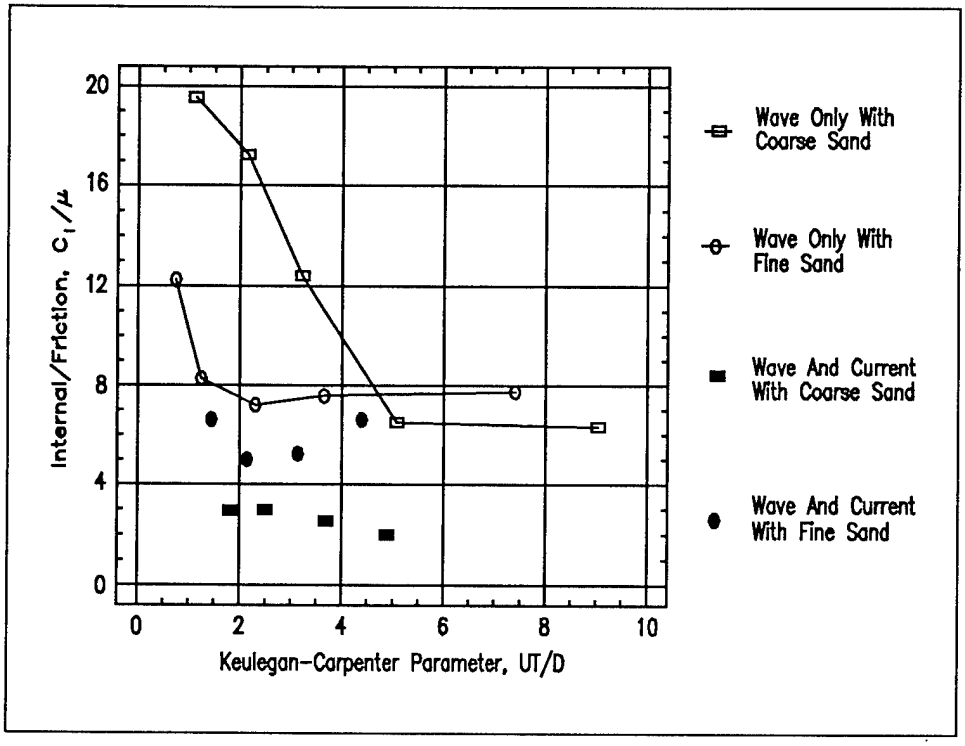

Figure 12. Inertia-friction coefficient ratio relative to Keulegan-Carpenter parameter

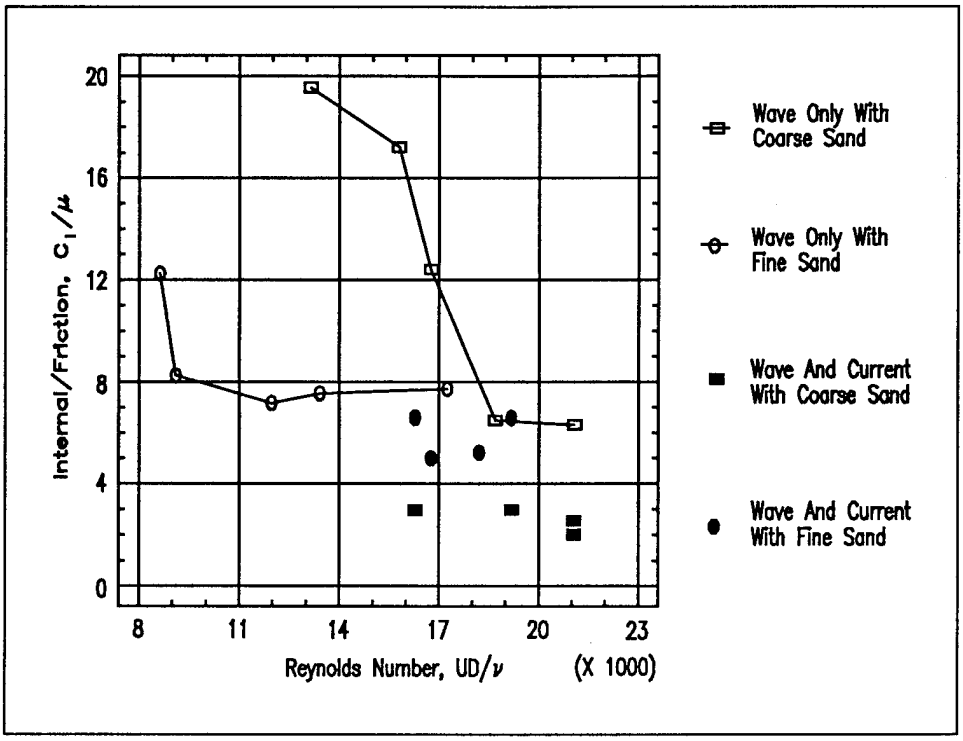

Figure 13. Inertia-friction coefficient ratio relative to Reynolds number

Figure 8 resolves the grain size and current effects on the threshold-to-fall velocity ratio (*utb/uf*) as different functions of the Keulegan-Carpenter parameter. Trends toward increasing velocity ratios with increasing Keulegan-Carpenter parameter are imposed by use of the same threshold velocity in the numerator of both ordinate and abscissa parameters. Lines added to this and the following plots are intended to help the reader identify trends within each grain size/current case because some points from different cases fall on top of each other. The peak speed (from the higher frequency wave oscillation) is used to calculate the Keulegan-Carpenter parameter. Only the shorter period wave was used to characterize the frequency because the longer wave simulated the superimposed current.

In Figure 9, the same ratio is graphed as a function of the Reynolds number. A similar scatter, weak correlation, and divergent relationships for the four principal grain size/current cases are again evident.

Dimensionless Drifter Weight Relationships

Figure 10 examines the drag-to-friction coefficient of Equation 2 as a function of the Keulegan-Carpenter parameter. As the Keulegan-Carpenter parameter increases, the drag force coefficient decreases, much like drag behavior on cylinders and spheres. Note that similar smooth curves could be fit to the points for each of the four listed conditions. While not coincident, the fit

curves would have similar shapes. To evaluate the Keulegan-Carpenter parameter, the SBD cap diameter D was again used as the characteristic length scale. The characteristic speed was the peak speed measured at the elevation of the SBD cap, 16.5 in. above the seabed. This speed is tabulated in Table A2 as wave velocity amplitude at the top of the seabed drifter (16 in. above bed) at threshold conditions (length/time), *uts*.

Generally, the "Wave Only with Coarse Sand" thresholds yielded larger drag force ratios than the "Wave Only with Fine Sand" threshold. This confirms that coarser bed materials (with higher threshold velocities) require heavier SBD weights to maintain equilibrium. The SBD's respond to the "Wave and Current with Coarse Sand" threshold with appreciably less drag than for "Wave Only with Coarse Sand" excitation. This current-induced difference is much less noticeable, however, in the case of "Fine Sand."

Figure 11 examines the same ratio of drag-to-friction coefficient, but now as a function of the Reynolds number. The results again follow the general trends of spheres and cylinders in that the drag coefficient decreases with an increasing Reynolds number for all four cases. For the "Wave Only" threshold, the "Coarser Sand" cases again display greater relative drag than the "Fine Sand" cases, but this distinction diminishes as the Reynolds number increases. The two sand sizes show reverse responses, however, to the superimposed current. The drag coefficient increases for the fine sand equilibrium and decreases for the coarse sand cases. Evidently the period in the Keulegan-Carpenter parameter introduces this effect instead of the velocity, which is common to the evaluation of both the Reynolds number and Keulegan-Carpenter parameter.

The lowest frequency "Wave and Current with Coarse Sand" produces, as expected, the smallest relative drag. From the records, it does not appear that there was any change in the Reynolds number for this lowest drag run compared to the previous run with the next-to-lowest drag. The Reynolds numbers are the same because the recorded peak velocities were identical (6.11 in./sec). If the velocity did increase for the longer wave length, as might be expected from theory, the lowest drag point should be shifted to the right, which could continue the trend shown by the other runs. In any case, uncertainties at this low end of the drag coefficient range are visually magnified by the semi-log scale in Figure 11.

Figure 12 shows how the inertial-to-friction coefficient (which comes from transposing terms in Equation 6, and is tabulated in Table A3) varies as a function of the Keulegan-Carpenter parameter. The inertial coefficients are larger and less variable than the drag coefficients, but display similar patterns. Inertial coefficients decrease with an increasing Keulegan-Carpenter parameter. As with "Wave Only" drag conditions, the "Coarse Sand" thresholds yield the highest force coefficients and the introduction of a current reduces the force coefficients for both sand sizes. Again, as with the drag ratio, the current had a greater effect on the "Coarse Sand" cases.

Figure 13 presents the same inertial-to-friction coefficient as a function of the Reynolds number. Again, coefficients tended to decrease as the Reynolds number increases, just as with the increasing Keulegan-Carpenter parameter. This behavior is similar to that of cylinders and spheres in the post-critical Reynolds number range, where the wake behind the object starts to increase in size. Also the "Wave Only with Coarse Sand" case again yielded the largest force coefficients. This suggests that higher threshold velocities and accelerations require more than proportional increases in the SBD weight to maintain equilibrium. Superimposing the current reduced the inertial coefficient ratio, and this effect was greater for "Coarse Sand" than for "Fine Sand" cases.

Summarizing the common features of Figures 10 to 13, the ratio of the displacing force on the SBD (either inertial or drag) to the restraining force (bed friction) decreased smoothly as Reynolds numbers and Keulegan-Carpenter parameters increased. This held true for all 16 combinations of currents, sand sizes, and ways of characterizing the displacement force. The ratios were measurably different for most of the 16 combinations, but displayed similar functional dependances on Reynolds number and the Keulegan-Carpenter parameter. The force ratios were largest for the "Wave Only with Coarse Sand" condition. The effect of adding a mean current tended to reduce this ratio (with only 1 exception out of 16) and a superimposed current had a greater effect for "Coarse Sand" conditions.

Resolving the wave and current components would be desirable. A Fourier analysis of the velocity records would reveal the velocity amplitude of both frequency components. These could be summed to provide the extreme seabed velocity and a weighted Keulegan-Carpenter parameter could be obtained from the sum of the products of the velocity amplitude and period. This type of analysis is not possible with the present data because analog oscillograph records were used to record the velocity data for these tests.

5 Discussion

Grain Size and Bed Form Effects on Sediment Threshold Velocities

Measured sand threshold velocities corresponded with available theory on motion initiation under oscillatory flow. Trends observed in this study were similar to those reported from flat-bed experiments, but incipient motion occurred at slower speeds. For steady flow, Menard (1950) observed that bed forms reduced threshold velocities 25 to 12 percent below flat beds. Rathbun and Goswami (1966) observed that ripples on a 0.3-mm sand bed lowered the threshold 54 percent. Based on Lofquist's (1975, 1978) oscillatory flow tunnel results, Hallermeier (1980) suggests sand should be entrained from ripple crests at peak speeds about half those for flat beds. As seen in Figure 6, predicted thresholds for flat beds were *on the average* 50 percent larger than measured over the equilibrium ripples. Individual percentages, however, were greater for the lower speeds and less for the higher speeds. Over the range tested, these differences are much better expressed as a simple constant rather than a proportional increase in threshold speed. All observed critical speeds for entrainment from the ripple crests were about 1.6 in./sec (4 cm/sec) lower than expected for flat beds using Equation 14. The data and a simple offset prediction equation are shown in Figure 14.

No known theory quantitatively accounts for bed form effects on sand threshold velocities. Though not an intended aspect of this SBD study, it is noteworthy that the 1.6 in./sec offset held reasonably well for the sand and ripple sizes tested over a threefold increase in threshold velocities. Additional data are needed to see if such a constant could be a useful rule of thumb for transposing plane-bed predictions to real-world, near-equilibrium bed form conditions.

As seen in Figure 15, a similar offset would approximate the tested grain size differences (going from d_{50}'s of 0.21 to 0.33 mm), especially for the combined wave and current conditions. An offset of 1.4 in./sec would be a better fit for the overall data, but the distinction is not justified for the limited data set. Here also, the meager data provide less support for dismissing a

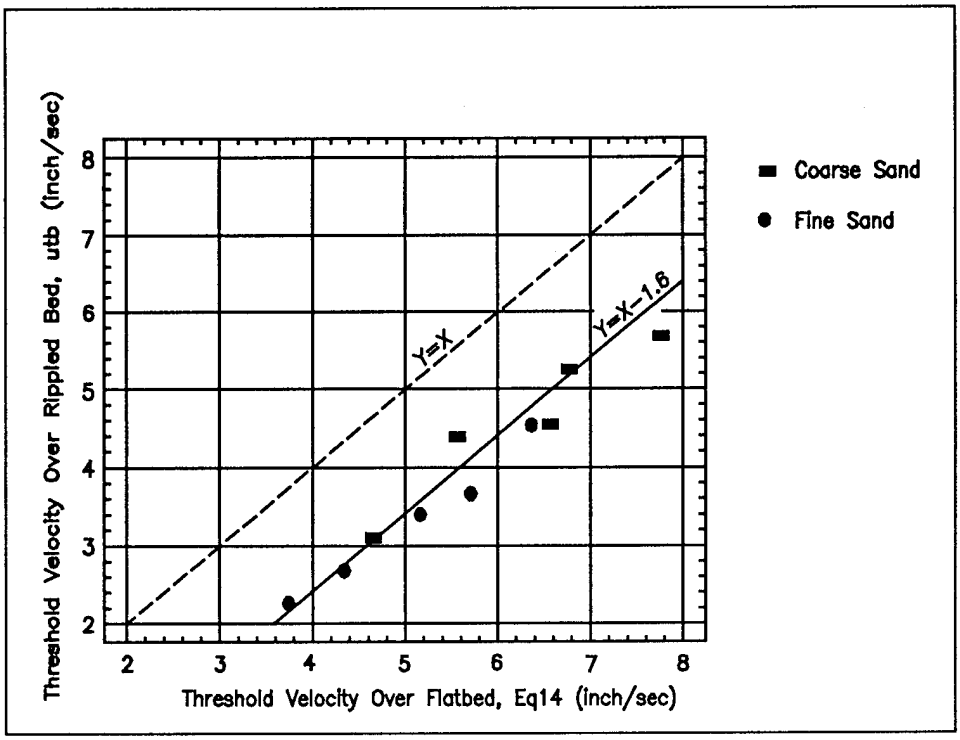

Figure 14. Bed form effect on threshold velocities

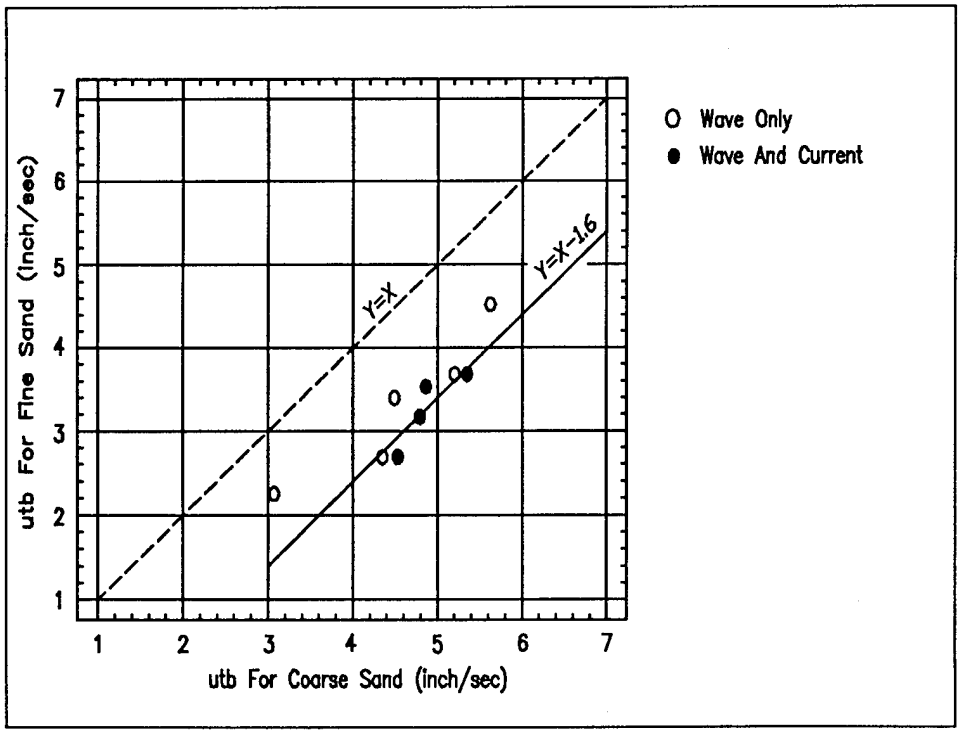

Figure 15. Grain size effect on threshold velocities

slope (multiplication) factor, but there is another argument for doing so. Hallermeier (1980) shows that for large Keulegan-Carpenter values and a thoroughly mixed rather than laminar boundary layer, the theoretical threshold velocities can be simplified to the following frequency-free expression:

$$U = \left(8\frac{\rho_s-\rho}{\rho}g\ d_{50}\right)^{0.5} \qquad (15)$$

where

ρ = density of sediment grains (mass/(length)^3)

The form of this equation does support expressing the difference in threshold velocities for any two grain sizes as a constant, independent of wave frequency and relative depth.

$$U_C - U_F = \sqrt{8\frac{\rho_s-\rho}{\rho}g}\quad\left(\sqrt{d_{50C}}-\sqrt{d_{50F}}\right) \qquad (16)$$

Evaluating Equation 16 for the 50 °F freshwater and quartz density provides essentially the same value observed on the rippled floor of the wave tank:

$$U_C - U_F = \sqrt{8\times1.65\times9807\frac{mm}{\sec^2}}\quad\left(\sqrt{0.33\,mm}-\sqrt{0.21\,mm}\right)\times(1\ in/2.54\ mm)$$

$$= 1.6\ in/\sec$$

Figure 15 shows that differences in critical velocities for the nine "Coarse Sand" cases and the nine "Fine Sand" cases that were exposed to the same set of wave frequencies closely match the 1.6 in./sec difference predicted by Hallermeier's mixed boundary layer expression (Equation 15). Measurements agree with predictions even though the grain sizes were not large enough by themselves to assure thorough mixing of the boundary layer. Accordingly, Hallermeier's (1980) criterion for negligible viscous effects in the laboratory is, as he intended, overly conservative for large-scale and field applications where ripples and other irregularities presumably create sufficient turbulence to justify use of Equation 15 in the field. The close agreement between observations and Equation 15 also indicates a level of consistency between these full-scale laboratory appraisals of incipient motion and Hallermeier's synthesis of a large number of previous experimental data sets.

Though the range of conditions observed here was limited, it seems noteworthy that the superposition of a substantial current in about half the runs (solid symbols in Figure 15) had no significant effect on the simple offset supported by the "Wave Only" cases. Over the last half century, much more data has been collected on thresholds under steady rather than under unsteady flow; and more recent work on oscillatory flow far exceeds experiments under combined oscillatory and steady flow. Hammond and Collins (1979) studied sediment thresholds on an oscillating bed suspended in a steady flow, but only for flat bed situations. Wave tunnel experiments over rippled beds were conducted by Nakato et al. (1977) for oscillatory flow, Arnott and Southard (1990) and Young and Sleath (1990) for combined flow, but did not include data on motion initiation. No reports are known comparing the effect of ripples on lowering the threshold of motion under oscillatory as compared to combined flow conditions.

Responses of Seabed Drifters and Effect of Varying Weights

Even though this study involved only two sediment sizes (d_{50}= 0.33 and 0.21 mm), the results clearly show that equilibrium weighting depends heavily on the grain size being mimicked. Although the equilibrium weightings for both sand sizes were very similar for high Reynolds numbers, they diverged as flow intensities decreased. The 30-percent reduction in median grain diameter yielded about a 50-percent reduction in the equilibrium weighting for "Fine Sand" conditions under the lower tested Reynolds and Keulegan-Carpenter numbers.

The SBD responses showed good correspondence with the well-known hydrodynamic responses of simple shapes. The equilibrium weighting of an SBD is sensitive to the wave period. The effects of period are not the same on SBD's and sands. As the wave changes from relative deepwater conditions to near shallow water, the equilibrium weight decreases by a factor of 4 for the relatively coarse sediment and by a factor of 2.5 for the relatively fine sediment. The drag and inertial coefficient dependence on Reynolds number and the Keulegan-Carpenter parameter correspond to the behavior of isolated spheres and cylinders, confirming that the SBD trends are consistent with known small-body hydrodynamic concepts. The dependence of force coefficients on flow conditions is more revealing in terms of Reynolds and Keulegan-Carpenter numbers (Figures 10-13) than threshold-to-fall velocity relationships (Figures 8 and 9) and follows a family of smooth curves related to the grain size and the presence or absence of mean currents. These dependencies can be used to estimate approximate equilibrium weightings and to compare initiation of motion between SBD's and sediment if the design conditions can be parameterized.

Clearly, a single ferrule weight crimped to the stem of an SBD will not provide equilibrium weightings valid over a wide range of sediment sizes and wave periods. A range of specific ferrule weights would be necessary to cover different field conditions.

6 Examples of Applications

Relationships developed herein can be used to calculate which grain sizes might have been entrained by conditions that were not energetic enough to move SBD's. Alternatively, they can be used to estimate grain sizes that might have remained in place while lightly weighted SBD's moved under weak flow. Prior to deploying SBD's, these relationships should be used to select ferrule weights so that SBD's mimic the threshold of the grain size of interest. These procedures can be confidently applied, however, only within the range of sediment sizes (0.21 mm $\leq d_{50} \leq$ 0.33 mm) and (less restrictive) relative water depths ($0.12 \leq 4\pi^2 h/gT^2 \leq 3.14$) covered by the experimental data reported here. Figures 10 to 13 permit quick visual assessment of the scatter, the potential effects of superimposed currents and different grain sizes.

Consider the required ferrule weight to simulate incipient motion for a 0.2-mm sand in a water depth of 52 ft experiencing an 8-sec wave period. This material corresponds to the "Fine Sand" case examined in this study (d_{50} = 0.21 mm). To find the appropriate ferrule weight, the following steps are required:

a. Evaluate the threshold velocity from measured curves in Figure 5 or by adding 1.6 in./sec (4 cm/sec) to results from Equation 14 or 15.

b. Evaluate the drag-friction coefficient ratio from Figure 10 or 11.

c. Solve for the submerged SBD weight by inverting Equation 2.

d. Solve Equation 7 for the net weight of the metal ferrule.

Evaluate Threshold Velocity from Figure 5

The abscissa of Figure 5 requires the linear wave theory, deepwater wave length L_0, which is obtained from the dispersion equation:

$$L_0 = \frac{g}{2\pi}T^2 = \left(\frac{32.2 ft/sec^2}{2\pi}\right)(8\,sec)^2 = 328 ft$$

The deepwater nondimensional wave number is:

$$\frac{2\pi h}{L_0} = \frac{2\pi(52 ft)}{328 ft} = \frac{327}{328} = 0.997$$

$$\cong 1.0$$

which is well within the experimental range of the data, so Figure 5 is entered at a value of unity on the abscissa to find a threshold velocity value of 3.0 in./sec for the measured velocities on "Measured Fine Sand." Thus,

U = 3 in./sec = 0.25 ft/sec (7.6 cm/sec)

Evaluate Drag-Friction Coefficient Ratio from Figure 10 or 11

Figure 10 requires the K-C parameter UT/D. Characteristic length D is the cap diameter:

D = 7.0 in. = 0.583 ft

Then,

$$\frac{UT}{D} = \frac{(0.25 ft/sec)(8\,sec)}{0.583 ft} = 3.43$$

Note the "Wave Only with Fine Sand" results in Figure 10. Entering the abscissa at a Keulegan-Carpenter parameter of 3.43 provides an intercept for the "Wave Only with Fine Sand" condition at a drag-friction coefficient ratio of:

$$\frac{C_D}{\mu} = 0.40$$

An alternate value for this ratio is provided relative to the Reynolds number in Figure 11. Assuming an open-water temperature of 60 °F, the kinematic viscosity would be 1.22 x 10-5 ft^2/sec, and the Reynolds number becomes:

$$\frac{UD}{\nu} = \frac{(0.25 ft/sec)\,(0.583 ft)}{1.22\times10^{-5} ft^2/sec} = 1.19 \times 10^4$$

By referring to "Wave Only with Fine Sand" in Figure 11, entering the abscissa at the calculated Reynolds number and intercepting the "Wave Only" data provides a drag-friction coefficient ratio of:

$$\frac{C_D}{\mu} = 0.42$$

Even if these two estimates of the drag ratio had not been in such close agreement, the wave frequency effect in the Keulegan-Carpenter parameter could be considered as equally important to the viscous effect in the Reynolds number; in which case the two different estimates of the drag ratio (from Figures 10 and 11) should be averaged to provide in this example:

$$\frac{C_D}{\mu} = \frac{0.40+0.42}{2} = 0.41$$

Solve for Submerged Weight of the SBD from Equation 2

Inverting Equation 2 for W provides:

$$W = \frac{C_D}{\mu}\frac{\rho A U^2}{2} = \frac{C_D}{\mu}\frac{\gamma}{g}\frac{\pi D^2}{4}\frac{U^2}{2}$$

$$= (0.41)\left(\frac{62.4\,lb/ft^3}{32.2\,ft/\sec^2}\right)\frac{\pi}{4}(0.583ft)^2\frac{(0.25ft/\sec)^2}{2}$$

$$= 0.00663\,lb$$

The mass of this assembled SBD would be

$$M = 0.00663\,lb\ (453.6\,g/lb) = 3.00\,grams$$

Solve Equation 7 for Weight of the Metal Ferrule

Solve Equation 7 for the weight of the metal ferrule W_f. The experimentally determined buoyancy of the test SBD's without the ferrule was 0.00661 lb, so

$$W_f = W - (-0.00661) = 0.00663 + .00661 = .0132 \text{ lb}$$

This weight would be equivalent to a 6-gram mass and close to that which oceanographers commonly use. For SBD's composed of plastic with a different specific gravity, with a sonic tag attached, or even with an attached information card that could change the composite SBD density, a new buoyancy value should be determined and, strictly speaking, adjusted for the salinity and temperature of waters in which those SBD's would be deployed.

In this example, it is concluded that a .0132-lb ferrule is required to properly simulate threshold movement of a 0.2-mm sand exposed to an 8-sec wave in a freshwater depth of 52 ft.

The large volume of the SBD compared with a sand grain means that heavier weights are necessary in salt water as opposed to freshwater to provide equilibrium with the same grain size material. If the previous problem had been for the open marine environment, the specific weight of seawater would have been used to evaluate Equation 2. Assuming full 35-ppt salinity and a temperature of 60 °F (15 °C),

$$\gamma = 64.15\ lb/ft^3$$

Thus,

$$W = \frac{C_D}{\mu}\frac{\gamma}{g}\frac{\pi D^2}{4}\frac{U^2}{2}$$

$$W = (0.41)\left(\frac{64.15\,lb/ft^3}{32.2\,ft/\sec^2}\right)\frac{\pi}{4}(0.583\,ft)^2\frac{(0.25\,ft/\sec)^2}{2}$$

$$W = 0.00690\ lb$$

The equivalent mass would be

$$M = 0.00690\,lb\ (453.6\,grams/lb) = 3.13\,grams$$

The SBD buoyancy in 60 °F seawater without the metal ferrule would thus be about 4 percent greater than in the initial freshwater evaluation. Returning to Equation 7, the net mass of the ferrule should likewise also be greater, yielding a heavier SBD weight for the open coast application:

$$W_f = W + 0.00661\ (1.029) = 0.0069 + .0068 = 0.0137\ \text{lb}$$

Alternative Procedures

It is also possible to solve for the submerged weight of the SBD via the inertial-to-friction coefficient. But since the sediment is drag-dominated (as shown on page 4), it is recommended that the drag-to-friction coefficient be used, as in the preceding example.

Weights in Water and Air

All weights referred to thus far have been for objects submerged in water (the product of gravitational acceleration times the difference in densities of the object and fluid in which it is immersed). Changes in submerged weight of the assembled SBD as functions of water temperature and salinity were shown to have a maximum effect of about 3 percent. After determining the submerged ferrule weight W_f that provides the desired threshold weighting relationship, the ferrules could be ordered, and most conveniently described, by specifying their mass or weight in air.

After reviewing about 25 published SBD reports, Resio and Hands (1994) found that ferrule masses were reported to only the nearest gram. If changes in SBD weight with water density are to be considered, ferrule mass must be specified more precisely. The standard deviations of ferrule mass in several orders from two different commercial SBD suppliers were all near 0.15 gram. It is, therefore, feasible to specify typical ferrule mass a little more precisely. Several CERC field studies used ferrules cut from brass tubing. This procedure permitted efficient adjustment of SBD thresholds to different conditions; it also reduced variation in ferrule weight. The standard deviations were less than 0.03 gram.

The ratio of weight of an object in air to weight in water W'/W is equal to the ratio of the object's density ρ_o to the difference in densities between it and water $\rho_o - \rho$. Because ferrule density is much greater than plastic, differences in weight in water and air will be much less for the ferrule than for the plastic or the assembled SBD. CERC's brass tubing had a density of 8.5 gram/cm^3. Using 1.000 gram/cm^3 as the lower bound on density of the water in which SBDs will be used, the increase in ferrule weight for air versus water would be 13.3 percent. So, the difference is important. Using 1.03 gram/cm^3 as an upper bound density, the increase would be 13.8 percent. So, the variation in this difference due to changing water densities is negligible. In most cases increasing the calculated submerged weight by 13.5 percent would be more than satisfactory. Similar adjustments could be made for other metals. Densities of soft steel and copper are near 7.7 and 8.9 gram/cm^3, respectively.

7 Conclusions

Observed sediment threshold velocities in the wave tank averaged about 50 percent less than the velocities predicted using Komar and Miller's well-known (1973) equation. That equation, and the other known predictors, are based on flat bed experiments. Flat beds exist only briefly in most coastal environments, so for this experiment the tank was seasoned to produce equilibrium ripples for each run prior to introducing the SBD's. The effect of the bed forms in these tests is best described as a lowering of the near-bed threshold velocities by about 1.6 in./sec (4 cm/sec). The 1.6 in./sec lowering of speed happens to correspond to a 50 percent drop in threshold velocity for fine sand or a rippled bed subjected tp 3-sec waves.

No single definitive relationship was found relating SBD fall velocity and the velocity that would induce incipient motion for both the sand and the equilibrium weighted SBD because of a strong, frequency-dependent grain size effect.

The measured threshold velocities and submerged SBD weight can be combined, however, to yield nondimensional ratios of the drag-to-friction coefficients and inertial-to-friction coefficients as functions of the Keulegan-Carpenter parameter and Reynolds number of the flow. These force coefficients are shown here as a family of similar curves for each of 16 hydrodynamic conditions based on two ways of characterizing flow intensity, two parameterizations of the entraining force, two sand sizes, and two current conditions. Drag ratios varied from approximately 3 to 0.05, decreasing with an increasing Keulegan-Carpenter parameter and Reynolds number. The inertial coefficients ratios ranged from about 20 down to 2, also decreasing with an increasing Keulegan-Carpenter parameter and Reynolds number. These behavior patterns are similar to those of simple bodies, such as spheres and cylinders. Both coefficients are larger for coarser sand threshold conditions, in a manner similar to the increase in drag as roughness increases on a cylinder.

Superimposing a long wave or current on the shorter waves decreases the force coefficient ratios. The mean current increases the mean Reynolds number and turbulence level, causing a decrease in the force coefficients (similar to the reduction in the friction factor observed in pipe experiments). The effects of strong currents on both coefficients were greater for the "Coarser Sand" thresholds. Consequently, the force coefficients and equilibrium weightings

converge to similar values for higher Reynolds numbers and Keulegan-Carpenter parameters regardless of the sand size and presence or absence of a steady current.

Graphical relationships, developed in this initial investigation of how SBD's respond to waves and currents, can be used to estimate the ballast or stem weight necessary to simulate threshold conditions for specific limited sand sizes, and wave and current combinations. Not surprisingly, SBD weights should be increased to mimic larger grain size thresholds. The dependence is, however, complex and strongly affected by the wave frequency, and the presence or absence of a mean current or long wave, so that a single weighting cannot match all sand thresholds over a wide range of conditions. Within tested ranges, however, equilibrium weights appear less sensitive to variations in conditions when grain sizes are small, turbulence is high, or multiple-frequency currents exist.

Graphs presented here can be used to correlate SBD and sand thresholds for specific design waves either without a significant mean current or with a collinear current having a velocity approximately equal to half the near-bed threshold velocity. Heavier than conventional weights should be used in tracing sand movement so that the SBD's are not displaced until the sediment threshold is exceeded. When in motion, the heavier SBD's will also respond more like sand in terms of wave phases and gravitational settling. These heavier SBD's will respond less to wind-driven currents which Resio and Hands (1994) found to be the dominant force moving lighter SBD's off the Alabama coast.

Results presented here are based on controlled laboratory tests. Because nature is more random and chaotic, laboratory results tend to be conservative estimates of seafloor disturbances (i.e., results underestimate turbulence and sediment entrainment potential). This failure to model all effects could be somewhat mitigated in the present work because the goal was to examine SBD motion initiation *relative to* sand motion initiation. Both the SBD's and the sand were exposed to the same contrived forces. The developed methodologies relating SBD and sand thresholds are, however, limited to grain sizes ($0.21 \text{ mm} \leq d_{50} \leq 0.33 \text{ mm}$) and relative water depths ($0.12 \leq 4\pi^2 h/gT^2 \leq 3.14$) examined.

The aim in allowing the user to select representative forcing parameters from graphs is to convey the level of uncertainty appropriate for each particular application and the sensitivity of the results to grain size and current variations. The lines in Figures 10 to 13 help identify data types and suggest trends, but should not restrict the user's judgement when applying the results to intermediate conditions. Additional tests could expand the range of application and the confidence in results.

8 Recommendations for Field Deployments and Lab Studies

Field Deployment Recommendations

Variously weighted SBD's should be used in future field tests that monitor dredged material movement. Field results could verify correlation of recovery distributions for specific weights with movement of specific sediment sizes. Until field verified, the practicality of using SBD's, with wave-frequency sensitive thresholds, to forecast sediment fate under varying field conditions remains problematic.

Given the relatively low cost of SBD's and value of knowing current and sediment trajectories when trying to anticipate the long-term fate of placed materials, SBD's should be used to supplement all ongoing monitoring efforts.

Historically, oceanographic studies with SBD's used light stem weights that provided nearly neutral buoyancy. Thus weighted, SBD's moved with currents much as plankton and wash load moved. Most of these earlier field deployments used 6-gram or lighter stem weights (reviewed in Resio and Hands 1994). With SBD's from the only two known commercial sources, 6-gram stem weights would provide a slight negative buoyancy with no attached return card. The specific gravity of commercially available cards vary significantly. Some are denser than water, some are not. To assure that only a negligible number of the least dense SBD's float, the distributions of densities of assembled SBD's should be checked for each newly acquired batch of drifters. If the intent is to track bottom currents, examination of densities can not be safely neglected for stem weights below 7 grams.

In sediment applications, densities of the assembled SBD's should always be known. Heavier stem weights will usually be desirable to match a sand-motion threshold, especially for studies beyond breaker zone where currents can fall below sand-movement thresholds during parts of each wave phase and sometimes remain below threshold for day or weeks. Guidance developed in this report can be used to select stem weights based on sediment,

oceanographic, and project conditions. The heavier SBD's disperse more slower. Other factors being equal, a greater number of releases may be necessary to obtain meaningful results from field studies with heavier weighted SBD's.

Laboratory Studies Recommendations

Future laboratory tests should consider the following: Thresholds should be correlated to a greater range of sediment sizes. Apparently heavier SBD weights could simulate threshold conditions outside the range tested; however, testing five or more sediments would allow more definitive relationships to be drawn between equilibrium weightings and the combined effects of wave properties and sand grain size.

Combined waves and currents might be tested with slower relative currents, especially for fine sand, to obtain a clearer picture of grain-size sensitivity under a range of realistic mixed-frequency flows.

Water depth should be varied in addition to the nondimensional wave number. This will allow examination of velocity gradients that may affect drag forces on the SBD cap differently from sand grains on the seabed.

Differences in the modes of SBD displacement, noted in the video documentation, deserve more attention in regards to the type and size of bed form plus the different modes of SBD movement across these bed forms. More explicit parameterization of lift may also be useful.

Threshold sediment velocity and SBD weights might be tested for some smooth bed cases. The resulting observations would serve as an extreme condition, contrasting with the equilibrium ripple results presented here. Conditions should be duplicated to maximize the utility of the two data sets.

Information on the directions of net transport for sand and SBD displacements with various combinations of mean and oscillatory velocities above the threshold conditions would be useful. All wave and current data should be digitally recorded to allow a frequency analysis and resolution of random and long wave/short wave simulations.

Laboratory studies allow control over the hydrodynamic conditions and repetition of important combinations of variables to reveal basic relationships. Because of the strong dependence on Reynolds number shown in this study, combined Froude and Reynolds modeling can only be done at near-prototype scale. A large number of releases under well-instrumented field conditions are necessary to verify practical application of laboratory results under variable real-world limitations.

References

Arnott, R. W., and Southard, J. B. (1990). "Exploratory flow-duct experiments on combined-flow bed configurations, and some implications for interpreting storm-event stratification," *Journal of Sedimentary Petrology* 60, No. 2, 211-19.

Bartolini, C., and Pranzini, E. (1977). "Tracing nearshore bottom currents with sea-bed drifters," *Marine Geology* 23, 275-84.

Chakrabarti, S. K. (1991). "Wave forces on offshore structures." *Handbook of Coastal and Ocean Engineering*. J. B. Herbich, ed., Gulf Publ. Co., Houston, TX.

Collins, M. B., and Barrie, J. V. (1979). "The threshold of movement of the Woodhead sea-bed drifter under unidirectional and oscillatory flows separately and in combination," Department of Oceanography, University College of Swansea, Swansea SA2 8PP, S. Wales, United Kingdom.

Dean, R. G. (1974). "Evaluation and development of water wave theories for engineering application," Special Report No. 1, Vol II, Coastal Engineering Research Center, U.S. Army Engineer Waterways Experiment Station, Vicksburg, MS.

Folger, D. W. (1971). "Nearshore tracking of seabed drifters," *Limnol. Oceangogr.* 16, 588-9.

Fredette, T. J., Clausner, J. E., Hands, E. B., Adair, J. A., and Sotler, V. A. (1990). "Guidelines for biological and physical monitoring of aquatic dredged material disposal sites," Technical Report D-90-11, U.S. Army Engineer Waterways Experiment Station, Vicksburg, MS.

Goda, Y., and Suzuki, Y. (1976). "Estimation of incident and reflected waves in random wave experiments." *Proceedings, 15th International Conference on Coastal Engineering*. Vol I, Honolulu, HI, 828-45, ASCE, New York.

Gross, M. G., Morse, B., and Barnes, C. A. (1969). "Movement of near-bottom waters on the continental shelf off the northwestern United States," *Journal of Geophysical Research* 74, 7044-47.

Hallermeier, R. J. (1980). "Sand motion initiation by water waves: Two asymptotes," *Journal of the Waterway, Port, Coastal and Ocean Division* 106 (WW3), 299-318. (Also Reprint 80-3, Coastal Engineering Research Center, U.S. Army Engineer Waterways Experiment Station, Vicksburg, MS).

Hammond, T. M., and Collins, M. B. (1979). "On the threshold of sand-sized sediment under the combined influence of unidirectional and oscillatory flow," *Sedimentology* 26, 795-812.

Hands, E. B. (1987). "Potential of seabed drifters for nearshore circulation studies." *Proceedings, Coastal Sediments' 87.* New Orleans, LA, ASCE, New York, 865-80.

Hands, E. B., and Cox, C. R. (1994). "Revision of Oregon State wave tank data on threshold conditions for seabed drifters," Memorandum for Record, Coastal Engineering Research Center, U.S. Army Engineer Waterways Experiment Station, Vicksburg, MS.

Harvey, J. (1968). "The movement of sea-bed and sea-surface drifters in the Irish Sea 1965-1967," *2nd European Symposium on Marine Biology.* Sarsia, 34, 227-42.

Hicks, L. L. (1986). "Siuslaw sea bed drifter study," U.S. Army Engineer District, Portland, OR.

King, D. B., Jr. (1991). "Studies in oscillatory flow bedload sediment transport," University of California, San Diego, CA.

Komar, P. D., and Miller, M. C. (1973). "The threshold of sediment movement under oscillatory water waves," *Journal of Sedimentation Petrology* 43, 1101-10.

Lee, A. J., Bumpus, D., and Lauzier, L. (1965). "The sea-bed drifter," *International Commission Northwest Atlantic Fish Bulletin* 2, 42-7.

Lofquist, K. E. B. (1975). "An effect of permeability on sand transport by waves," Technical Memorandum 62, U.S. Army Engineer Waterways Experiment Station, Coastal Engineering Research Center, Vicksburg, MS.

_____. 1978. "Sand ripple growth in an oscillatory-flow water tunnel," Technical Paper 78-5, U.S. Army Engineer Waterways Experiment Station, Coastal Engineering Research Center, Vicksburg, MS.

Menard, H. W. (1950). "Sediment movement in relation to current velocity," *Journal of Sedimentary Petrology* 20(3), 148-60.

Morison, J. R., O'Brien, M. P., Johnson, J. W., and Shaff, S. A. (1950). "The force exerted by surface waves on piles," *Petroleum Transactions*, AIME, 189, 149-154.

Nakato, T., Locher, F. A., Glover, J. R., and Kennedy, J. F. (1977). "Wave entrainment of sediment from rippled beds," *American Society of Civil Engineers Journal of Waterway, Port, Coastal, and Ocean Division* 103, No. WW1, 83-99 (also Reprint 77-5, U.S. Army Engineer Waterways Experiment Station, Vicksburg, MS).

Pape, E., and Garvine, R. (1982). "Subtidal circulation in Delaware Bay and adjacent shelf waters," *Journal of Geophysical Research* 87, 7955-70.

Phillips, A. W. (1970). "The use of the Woodhead sea bed drifter," British Geomorphological Research Group, Technical Bulletin No. 4., Kensington Core, London.

Rathbun, R. E., and Guy, H. P. (1967). "Measurement of hydraulic and sediment transport variables in a small recirculating flume," *Water Resources Research* 3(1), 107-22.

Resio, D. T., and Hands, E. B. (1994). "Understanding and interpreting seabed drifters," Technical Report DRP-94-1, U.S. Army Engineer Waterways Experiment Station, Coastal Engineering Research Center, Vicksburg, MS.

Riley, J. D., and Ramster, J. W. (1972). "Woodhead seabed drifter recoveries and the influence of human, tidal and wind factors," International Council for the Exploration of the Sea, *Journal Du Conseil* 34, 389-415.

Sarpkaya, T., and Isaacson, M. (1981). *Mechanics of wave forces on offshore structures*. Van Nostrand Reinhold, NY.

Schuldt, D. A. (1981). "Grays Harbor, Washington, preliminary results of surface/bottom drifter release study," U.S. Army Engineer District, Seattle, WA.

Sleath, J. F. A. (1984). *Sea bed mechanics*. John Wiley & Sons, New York.

Sollitt, C. K. (1990). "Threshold conditions for seabed drifters in wave and wave/current environments," unpublished contractor report, Dredging Research Program, U.S. Army Engineer Waterways Experiment Station, Coastal Engineering Research Center, Vicksburg, MS.

Sternberg, R. W., and Marsden, M. A. H. (1979). "Dynamics, sediment transport, and morphology in tide dominated Embayment," *Earth Science Processes* 4, 117-39.

Woodhead, P. M. J., and Lee, A. J. (1960). "A new instrument for measuring residual currents near the sea-bed," *International Council for Exploration of the Sea* 12.

Young, J. S. L., and Sleath, J. F. A. (1990). "Ripple formation in combined transdirectional steady and oscillatory flow," *Sedimentology* 37, 509-16.

Appendix A
Test Conditions and Results

These data were collected in the large wave tank at Oregon State University by staff of the O. H. Hinsdale Wave Research Laboratory under the direction of Dr. Charles K. Sollitt. The original data are reported in Sollitt (1990). Subsequent reanalysis of the data led to the data revisions used in this report. Complete data are given in the following three tables. Explanations for the revisions are given in Hands and Cox (1994).

Table A1
Wave Conditions

Run Number freq	Dean's Stream Case	T sec	L ft	Wave Envelope Method				Goda Method			
				H_{max} in.	H_{min} in.	H_I in.	R	H_{Ig} in.	H_{rg} in.	R_g Wave	R_g Wave & Current
2	8	2.07	21.92	24.32	21.76	23.04	0.06	22.25	1.93	0.09	
1	7	3.28	48.87	8.32	7.36	7.84	0.06	8.04	0.23	0.03	
3	6	4.63	78.01	8.80	7.36	8.08	0.09	7.69	0.78	0.10	
4	5	6.55	116.82	5.92	5.44	5.68	0.04	5.80	0.20	0.03	
5	4	10.36	190.87	6.88	4.64	5.76	0.19	5.24	1.22	0.23	
6 (lo)		10.42	182.32					2.50	0.55		0.22
6 (hi)		2.59	33.48					1.37	0.72		0.53
7 (lo)		10.42	182.32					3.13	0.55		0.18
7 (hi)		3.07	44.65					5.74	0.63		0.11
8 (lo)		10.42	182.32					3.14	0.59		0.19
8 (hi)		4.15	68.81					3.30	0.18		0.05
9 (lo)		10.42	182.32					3.02	0.68		0.23
9 (hi)		5.52	98.02					4.68	0.49		0.10
10	8	2.07	21.92	17.26	14.72	16.00	0.08	16.11	0.30	0.02	
11	7	3.28	48.87	5.44	4.16	4.80	0.13	5.05	0.83	0.16	
12	6	4.63	78.01	5.44	4.48	4.96	0.10	4.56	0.54	0.12	
13	5	6.55	116.82	4.80	4.48	4.64	0.03	4.38	0.36	0.08	
14	4	10.36	190.87	5.26	3.22	4.25	0.24	4.82	0.99	0.21	
15 (lo)		10.42	182.32					2.46	0.17		0.07
15 (hi)		2.13	23.06					10.91	0.14		0.01
16 (lo)		10.42	182.32					2.36	0.43		0.18
16 (hi)		3.07	44.65					4.98	0.48		0.10
17 (lo)		10.42	182.32					2.56	0.53		0.21
17 (hi)		4.15	68.81					2.24	0.08		0.04
18 (lo)		10.42	182.32					2.51	0.52		0.21
18 (hi)		5.52	98.02					3.70	0.48		0.13

Table A2
Near-Bed Hydrodynamics

Run Number freq	Dean's Stream Case	utb in./sec	Ub in./sec	up in./sec	up/utb in./sec	uts in./sec	Us in./sec	Deepwater Wave No. kh	Fall Vel. uf in./sec	ut/uf
2	8	3.11	-4.65	4.65	1.50	3.61	-1.39	3.15	6.60	0.47
1	7	4.39	0.00	5.55	1.23	4.58	-0.28	1.25	2.91	1.51
3	6	4.53	-0.28	6.57	1.26	4.86	0.00	0.63	1.84	2.46
4	5	5.24	0.00	6.77	1.56	5.42	0.00	0.31	1.19	4.40
5	4	5.66	0.00	7.76	1.38	6.11	0.00	0.13	1.02	5.55
6 (lo)		4.53				4.72		0.12	1.19	3.81
6 (hi)		4.53				4.72		2.01	1.19	3.81
7 (lo)		4.79				5.56		0.12	1.19	4.03
7 (hi)		4.79				5.56		1.43	1.19	4.03
8 (lo)		4.86				6.11		0.12	1.02	4.76
8 (hi)		4.86				6.11		0.78	1.02	4.76
9 (lo)		5.35				6.11		0.12	0.86	6.22
9 (hi)		5.35				6.11		0.44	0.86	6.22
10	8	2.26	-1.13	3.78	1.71	2.50	-1.11	3.15	1.98	1.14
11	7	2.69	0.00	4.37	1.67	2.64	0.00	1.25	1.42	1.89
12	6	3.40	0.00	5.20	1.56	3.47	-0.28	0.63	1.19	2.86
13	5	3.68	-0.14	5.75	1.60	3.89	0.28	0.31	1.10	3.35
14	4	4.53	0.00	6.42	1.45	5.00	-0.42	0.13	1.02	4.44
15 (lo)		2.69				4.72		0.12	1.68	1.60
15 (hi)		2.69				4.72		2.98	1.68	1.60
16 (lo)		3.17				4.86		0.12	1.46	2.17
16 (hi)		3.17				4.86		1.43	1.46	2.17
17 (lo)		3.53				5.28		0.12	1.42	2.49
17 (hi)		3.53				5.28		0.78	1.42	2.49
18 (lo)		3.68				5.56		0.12	1.42	2.59
18 (hi)		3.68				5.56		0.44	1.42	2.59

Table A3
Equilibrium Response Characteristics

Run Number freq	Dean's Stream Case	Brass Ferrule Mass grams	C_D/μ				C_I/μ				Reynolds No.	K-C Parameter
			Wave Only		Wave and Current		Wave Only		Wave and Current			
			Coarse	Fine	Coarse	Fine	Coarse	Fine	Coarse	Fine		
2	8	31.30	2.59				20.64				12,446	1.07
1	7	21.90	1.07				17.23				15,790	21.5
3	6	13.20	0.52				12.39				16,755	3.21
4	5	7.20	0.17				6.51				18,686	5.07
5	4	5.90	0.09				6.33				21,065	9.04
6 (lo)												
6 (hi)		7.20			0.23				2.96		16,273	1.75
7 (lo)												
7 (hi)		7.20			0.16				2.97		19,169	2.44
8 (lo)												
8 (hi)		5.90			0.09				2.54		21,065	3.62
9 (lo)												
9 (hi)		4.70			0.06				2.00		21,065	4.82
10	8	14.60		2.22				12.24			8,619	0.74
11	7	8.20		0.89				8.27			9,102	1.24
12	6	7.20		0.42				7.19			11,963	2.30
13	5	6.50		0.28				7.57			13,411	3.64
14	4	5.90		0.14				7.74			17,238	7.40
15 (lo)												
15 (hi)		14.50				0.62				6.62	16,273	1.44
16 (lo)												
16 (hi)		9.20				0.31				5.01	16,755	2.13
17 (lo)												
17 (hi)		8.20				0.22				5.23	18,203	3.13
18 (lo)												
18 (hi)		8.20				0.20				6.61	19,169	4.38

Appendix B
Notation

a	Amplitude of unsteady fluid acceleration = $\frac{2\pi U}{T}$ length/(time)^2]
A	Projected area of SBD (cap area) [length^2]
B	Orbital diameter of wave motion at seabed [length]
C_D/μ	Drag-to-friction coefficient at equilibrium conditions [dimensionless]
C_D	Drag coefficient [dimensionless]
C_I/μ	Inertial-to-friction coefficient at equilibrium conditions [dimensionless]
C_I	Inertial coefficient [dimensionless]
d	Diameter of a sphere [length]
d_{50}	Diameter of sediment grains [length]
D	Characteristic length (cap diam) [length]
F	Time-dependent, wave-induced longitudinal force [mass length/(time)^2]
F_D	Drag force on SBD [mass length/(time)^2]
F_I	Inertial force [mass length/(time)^2]
g	Acceleration due to gravity [length/(time)^2]
h	Water depth [length]
H	Wave height [length]

H_i Incident wave height from envelope = $(H_{max} + H_{min})/2$ [length]

H_{ig} Incident wave height by Goda's method [length]

H_{max} Antinodal height of wave envelope [length]

H_{min} Nodal height of wave envelope [length]

H_{rg} Reflected wave height by Goda's method [length]

I Ratio of force terms [dimensionless]

k Wave number = $\frac{2\pi}{L_o}$ [length $^{-1}$]

K-C Keulegan-Carpenter parameter [dimensionless]

L Wave length [length]

R Reflection coefficient of beach by envelope method [dimensionless]

R_e Reynolds Number [dimensionless]

R_g Reflection coefficient of beach by Goda's method [dimensionless]

T Wave period [time]

uf Terminal fall velocity of seabed drifter with brass ferrule attached [length/time]

up Predicted threshold velocity at the bed (Equation 14) [length/time]

utb Wave velocity amplitude 3 in. above bed at threshold conditions [length/time]

uts Wave velocity amplitude at top of seabed drifter (16 in. above bed) at threshold conditions [length/time]

U Sediment threshold velocity amplitude [length/time], (U_C - U_F = difference in threshold velocities for coarse and fine fraction)

Ub Mean velocity at seabed (positive referenced in direction of incident wave propagation) [length/time]

Us Mean velocity at top of seabed drifter [length/time]

V Volume of SBD = mass/density = $/\rho_d$ [length^3]

W	Submerged weight of assembled SBD [mass length/(time)^2]
W_d	Submerged weight (-1 × buoyancy) of SBD without any ballast
W_f	Submerged weight of metal ferrule [mass length/(time)^2]
γ	Specific weight of fluid surrounding SBD [mass/length^2 time^2]
γ'	Submerged weight of sediment per unit volume [mass/length^2 time^2]
μ	Friction coefficient between SBD and seabed [dimensionless]
ν	Kinematic viscosity of water [(length)^2/time]
π	Constant 3.14159 [dimensionless]
ρ	Density of water [mass/(length)^3]
ρ_d	Density of SBD [mass/(length)^3]
ρ_s	Density of sediment grains [mass/(length)^3]

REPORT DOCUMENTATION PAGE

Form Approved
OMB No. 0704-0188

1. AGENCY USE ONLY *(Leave blank)*	2. REPORT DATE	3. REPORT TYPE AND DATES COVERED
	December 1994	Final report

4. TITLE AND SUBTITLE
Correlating Seabed Drifter Weights to Sand Threshold Conditions in Wave and Wave/Current Environments

5. FUNDING NUMBERS
Work Unit 32467

6. AUTHOR(S)
Edward B. Hands, Charles K. Sollitt

7. PERFORMING ORGANIZATION NAME(S) AND ADDRESS(ES)
U.S. Army Engineer Waterways Experiment Station, 3909 Halls Ferry Road, Vicksburg, MS 39180-6199
Oregon State University, Corvallis, OR 97331

8. PERFORMING ORGANIZATION REPORT NUMBER
Technical Report DRP-94-7

9. SPONSORING/MONITORING AGENCY NAME(S) AND ADDRESS(ES)
U.S. Army Corps of Engineers
Washington, DC 20314-1000

10. SPONSORING/MONITORING AGENCY REPORT NUMBER

11. SUPPLEMENTARY NOTES
Available from National Technical Information Service, 5285 Port Royal Road, Springfield, VA 22161.

12a. DISTRIBUTION/AVAILABILITY STATEMENT
Approved for public release; distribution is unlimited.

12b. DISTRIBUTION CODE

13. ABSTRACT *(Maximum 200 words)*

The purpose of this study was to investigate the response of seabed drifters (SBD's) to combined waves and currents and, specifically, to examine the feasibility of modifying these bottom current drogues to behave more like sediment particles. This is the only known full-scale, quantitative study of the response of SBD's to wave and current forces. Standard design SBD's were modified by changing the attached weight so that the SBD's would move on the seafloor only when the flow conditions were sufficiently vigorous to initiate sediment motion. Relative drag and inertia coefficients for SBD's were evaluated and related to the Reynolds numbers and the Keulegan-Carpenter parameter. Using these relationships, a methodology was derived for selecting threshold SBD weightings appropriate for different situations.

The SBD's used in these tests were identical to those used in recently reported studies conducted by the U.S. Army Corps of Engineers at Duck, NC, Sand Island, AL, and Humboldt, CA.

14. SUBJECT TERMS

Bed forms	Drogues	Nearbed hydrodynamics	Seabed drifters
Bottom currents	Fate of open-water sediments	Onshore transport	Threshold velocity
Critical velocities	Motion initiation	Ripples	Tracers
Dredged material uses		SBD	Wave tank study

15. NUMBER OF PAGES
62

16. PRICE CODE

17. SECURITY CLASSIFICATION OF REPORT	18. SECURITY CLASSIFICATION OF THIS PAGE	19. SECURITY CLASSIFICATION OF ABSTRACT	20. LIMITATION OF ABSTRACT
UNCLASSIFIED	UNCLASSIFIED		